Title: Klf5 regulates muscle differentiation by directly targeting muscle-specific genes in cooperation with MyoD in mice

Research Article

Shinichiro Hayashi[1], Ichiro Manabe[2], Yumi Suzuki[1], Frédéric Relaix[3] and Yumiko Oishi[1*]

1- Department of Cellular and Molecular Medicine, Medical Research Institute, Tokyo Medical and Dental University, Tokyo, Japan

2- Department of Aging Research, Graduate School of Medicine, Chiba University, Chiba, Japan

3- INSERM U955 IMRB-E10 UPEC, ENVA, EFS, 8 rue du general Sarrail, 94010 Creteil - France

***Corresponding author:** Yumiko Oishi

Department of Cellular and Molecular Medicine, Medical Research Institute, Tokyo Medical and Dental University, Tokyo, Japan

19th floor of the M&D tower building,

1-5-45 Yushima, Bunkyo-ku, Tokyo 113-8510 Japan

Tel: +81-3-5803-4592

Fax: +81-3-5803-4978

Email: yuooishi-circ@umin.ac.jp

Abstract

Krüppel-like factor 5 (Klf5) is a zinc-finger transcription factor that controls various biological processes, including cell proliferation and differentiation. We show that Klf5 is also an essential mediator of skeletal muscle regeneration and myogenic differentiation. During muscle regeneration after injury (cardiotoxin injection), Klf5 was induced in the nuclei of differentiating myoblasts and newly formed myofibers expressing myogenin *in vivo*. Satellite cell-specific *Klf5* deletion severely impaired muscle regeneration, and myotube formation was suppressed in *Klf5*-deleted cultured C2C12 myoblasts and satellite cells. *Klf5* knockdown suppressed induction of muscle differentiation-related genes, including myogenin. Klf5 ChIP-seq revealed that Klf5 binding overlaps that of MyoD and Mef2, and Klf5 physically associates with both MyoD and Mef2. In addition, MyoD recruitment was greatly reduced in the absence of Klf5. These results indicate that Klf5 is an essential regulator of skeletal muscle differentiation, acting in concert with myogenic transcription factors such as MyoD and Mef2.

Impact statement

The regulatory programs governing skeletal muscle regeneration that are controlled by Klf5 in cooperation with MyoD and Mef2 provide a potential avenue for intervention into muscle regeneration through modulation of Klf5.

Key words:

Kruppel-like factor, Muscle regeneration, Muscle differentiation, Satellite cell

Submitting area(s):

Developmental biology & stem cells

Abbreviations:

SCs: Satellite cells

KLF: Krüppel-like factors

CRISPR: Clustered regularly interspaced short palindromic repeats

ChIP: Chromatin immunoprecipitation

TA: Tibialis anterior

EDL: Extensor digitorum longus

CTX: Cardiotoxin

MyHC: Myosin heavy chain

siRNA: small interfering RNA

RV: Retrovirus

Introduction

Skeletal muscle, the dominant organ for locomotion and energy metabolism, has a remarkable capacity for repair and regeneration in response to injury, disease and aging. Regeneration of adult skeletal muscle following injury occurs through the mobilization of satellite cells (SCs), a population of injury-sensitive quiescent muscle stem cells that activate, proliferate, differentiate, and fuse with injured myofibers. (Buckingham and Rigby, 2014; Relaix and Zammit, 2012). In an adult skeletal muscle, SCs, characterized by expression of the paired box transcription factor Pax7 are mitotically quiescent and reside in a niche between the basal lamina and sarcolemma of associated muscle fibers. In response to muscle damage, SCs are activated and assume a myoblast identity, thereby initiating muscle repair. After massive proliferation, SC-derived myoblasts undergo differentiation and fusion to form myotubes that replace the damaged myofibers (Comai and Tajbakhsh, 2014), while a subset of activated satellite cells downregulate MyoD, exit the cell cycle to replenish the muscle stem cell pool.

A large body of studies have shown that a family of four myogenic regulatory factors (MRFs) regulating early skeletal muscle development also regulate the postnatal muscle regeneration program. These MRFs include the myogenic basic-helix-loop-helix type transcription factors MyoD and Myf5, which are recruited to skeletal muscle-specific genes regulatory regions, where they determine myogenic fate and initiate the differentiation cascade. Thereafter, MyoD increases the expression of late target genes in cooperation with myogenin and MRF4 through a feed-forward regulatory mechanism that regulates terminal differentiation (Penn et al., 2004). MRFs also enhance myogenic activity by interacting with other transcription factors, including Mef2 (Fong and Tapscott, 2013; Molkentin and Olson, 1996).

Although the core MRF network that governs skeletal muscle regeneration and differentiation has been identified, the sequence of events within muscle-specific gene regulatory regions during differentiation is not fully understood. It is highly likely, for example, that the myogenic program driven by MRFs requires input from other transcription factors. More specifically, MRFs, including MyoD, may associate with other transcription factors that respond to microenvironmental cues and restrict the binding of MRFs to particular subsets of target enhancers. This would enable MRF complexes to context dependently regulate muscle genes governing the processes of myocyte differentiation and regeneration. Identification of these MRF partners is therefore important to clarify the mechanism by which MRF-containing transcriptional regulatory complexes achieve precise spatiotemporal regulation of their target genes.

Krüppel-like factors (Klfs) are a subfamily of zinc-finger transcription factors. All Klf proteins contain a DNA-binding domain consisting of three zinc fingers positioned at their carboxyl-terminal end, which enables their specific binding to “GT-box” or “CACCC” sites (Bieker, 2001). Several Klf members are involved in the control of skeletal muscle differentiation and function (Prosdocimo et al., 2015). For instance, Klf3 is upregulated during skeletal muscle differentiation and transactivates the muscle creatin kinase (*Mck*) promoter (Himeda et al., 2010). Klf2 and Klf4 are also upregulated in differentiating muscle cells and promote muscle cell fusion (Sunadome et al., 2011). Klf6 promotes and Klf10 inhibits myoblast proliferation (Dionyssiou et al., 2013; Parakati and DiMario, 2013). Klf15 critically regulates skeletal muscle nutrient catabolism, contributing to the regulation of exercise capacity and muscle wasting (Gray et al., 2007; Haldar et al., 2012; Shimizu et al., 2011). These studies demonstrate the pivotal involvement of Klfs in muscle biology. However, their role in the global

114 transcriptional program of muscle differentiation remains unclear. Interestingly, Cao et
115 al. previously showed that binding sites for Sp1, which is structurally related to Klfs and
116 binds to similar GC-rich sequences, are highly enriched in MyoD-binding regions,
117 which suggests there may be interaction between these two transcription factors.

118 Klf5 is reportedly involved in embryonic development (Shindo et al., 2002),
119 control of cellular proliferation and differentiation (Fujiu et al., 2005; Oishi et al., 2005),
120 stress response (Shindo et al., 2002), and apoptosis (Zhu et al., 2006). *Klf5* null embryos
121 fail to develop beyond the blastocyst stage *in vivo* or to produce embryonic stem cell
122 lines *in vitro*, indicating that Klf5 is essential for maintenance of stemness (Ema et al.,
123 2008; Shindo et al., 2002). Klf5 is expressed in many cell types, including gut epithelial
124 cells (Chanchevalap et al., 2004; Sun et al., 2001), vascular smooth muscle cells (Fujiu
125 et al., 2005), adipocytes (Oishi et al., 2005), neuronal cells (Yanagi et al., 2008) and
126 leukocytes (Yang et al., 2003). In smooth muscle cells, Klf5 regulates the genes
127 involved in early processes of differentiation, including SMemb/NMHC-B and SM22α
128 (Adam et al., 2000; Watanabe et al., 1999). Klf5 is also required for adipocyte
129 differentiation. In 3T3-L1 preadipocytes, Klf5 is induced at an early stage of
130 differentiation by C/EBPβ and δ, which is followed by expression of PPARγ_2 (Oishi et
131 al., 2005). We previously reported that Klf5 acts as a regulator of lipid metabolism in
132 skeletal muscle (Oishi et al., 2008). However, the role of Klf5 in skeletal muscle
133 differentiation has not been characterized. In the present study, therefore, we
134 investigated the role of Klf5 in skeletal muscle differentiation and regeneration.

Results

Klf5 is highly expressed in differentiating myoblasts during muscle regeneration

To test the hypothesis that Klf5 is involved in skeletal muscle regeneration, we first examined tibialis anterior (TA) muscle from C57BL/6J wild-type mice with and without cardiotoxin (CTX)-induced skeletal muscle injury (Lepper et al., 2009). As compared to expression in intact (uninjured) muscle, expression of *Klf5* mRNA in regenerating TA muscles was upregulated 2 and 4 days after injury, as was expression of myogenic factors (*Pax7*, *Myod1*, *Myog* and *Myh3*) (Figure 1A).

Our immunohistochemistry results showed that little or no Klf5 is expressed in Pax7-positive, quiescent SCs or myonuclei that constitute intact muscle (Fig. 1B upper panel, Figure1-figure supplement 1A). Seven days after CTX-induced muscle injury, we observed ongoing muscle degeneration characterized by the presence of centrally located nuclei in regenerating fibers. At that time, expression of Klf5 remained very low in Pax7-positive, activated SCs (Figure 1B, middle panel, arrows). However, higher levels of Klf5 were detected in differentiating myocytes, which expressed myogenin 7 days after injury (Figure 1B, lower panel, arrowheads). Klf5 was also detected within the centrally located nuclei of regenerating myofibers. These results indicate that Klf5 is markedly upregulated in differentiating myocytes and regenerating myofibers during the course of muscle regeneration *in vivo*.

To examine Klf5 expression during muscle differentiation *in vitro*, SCs were isolated from the extensor digitorum longus (EDL) muscle from wild-type mice and placed in culture. After the first passage, nearly 100% of cells were MyoD positive, confirming the high purity of the muscle cell cultures (Figure 1-figure supplement 1B,

C). Over 70% of the purified cells were also positive for Pax7 (Figure1- figure supplement 1C). Consistent with the *in vivo* results, little or no Klf5 was detected in a fraction of the activated SCs expressing Pax7 and MyoD (Figure 1C, upper panel). Approximately 75% of Pax7-positive cells were also weakly positive for Klf5 (Figure 1-figure supplement 1D). Klf5 was induced in differentiating myoblasts exhibiting an absence or low Pax7 expression (Figure 1C, arrows, Figure 1-figure supplement1D). After differentiation for 2 days, Klf5 was strongly expressed in the nuclei of differentiating myotubes and co-localized with myogenin (Figure 1C, middle panel, Figure 1-figure supplement 1E). However, the strong Klf5 expression was transient, and by day 4 of differentiation it was undetectable in the nuclei of larger, fused myotubes that had also lost myogenin expression (Figure 1C, arrowheads). These *in vitro* observations indicate that Klf5 is induced in differentiating myoblasts during muscle differentiation and then downregulated in mature myotubes.

Klf5 is required for muscle regeneration

The finding of temporal overlap between Klf5 expression and muscle regeneration and differentiation *in vivo* and *in vitro* prompted us to examine the role of Klf5 in SC-mediated muscle regeneration *in vivo*. Mice carrying floxed *Klf5* alleles with loxP sites were crossbred with mice expressing *Pax7*-driven CreERT2, a tamoxifen-inducible recombinase to generate $Pax7^{CE/+}$;$Klf5^{flox/flox}$ mice. The $Pax7^{CE/+}$ mice were previously shown to be able to ablate almost 100% of SCs when crossed with $R26R^{GFP\text{-}DTA/+}$ mice (Lepper et al., 2009; Lepper et al., 2011). The $Pax7^{CE/+}$;$Klf5^{flox/flox}$ model enabled us to selectively delete *Klf5* from SCs after tamoxifen injection. To induce SC-specific *Klf5* deletion, 8- to 12-week-old $Pax7^{CE/+}$;$Klf5^{flox/flox}$ mice were treated with tamoxifen for 5

183 days before use in subsequent experiments. Control *Pax7*$^{+/+}$;*Klf5*$^{flox/flox}$ mice were also
184 treated with tamoxifen. Hereafter, *Pax7*$^{CE/+}$;*Klf5*$^{flox/flox}$ and *Pax7*$^{+/+}$;*Klf5*$^{flox/flox}$ mice will
185 represent the mice treated with tamoxifen in this manner. Muscle histology revealed that
186 *Pax7*$^{CE/+}$;*Klf5*$^{flox/flox}$ mice or control *Pax7*$^{+/+}$;*Klf5*$^{flox/flox}$ mice displayed no obvious
187 phenotypic alterations under physiological conditions and exhibited no morphological
188 alterations in their skeletal muscle stained with hematoxylin and eosin (H&E) 28 days
189 after tamoxifen treatment (Figure 2-figure supplement 1).

190 After continuous tamoxifen administration for 5 days, CTX was injected into
191 the TA muscles of both *Pax7*$^{CE/+}$;*Klf5*$^{flox/flox}$ and control *Pax7*$^{+/+}$;*Klf5*$^{flox/flox}$ mice, which
192 were then analyzed 4, 7 and 28 days after injury. On day 4 after injury, mRNA
193 expression of *Myog* and *Myh3* was significantly lower in regenerating muscles from
194 *Pax7*$^{CE/+}$;*Klf5*$^{flox/flox}$ mice than control mice; *Pax7* and *Myod1* levels also tended to be
195 reduced, but the differences did not reach statistical significance (Figure 2A). On day 7
196 after injury, H&E and immunofluorescent staining in control mice revealed efficient
197 muscle regeneration characterized by regenerated myofibers with decreased expression
198 of eMyHC, a marker of immature myofibers (Fig. 2B). On the contrary, the regeneration
199 process was significantly impaired in *Pax7*$^{CE/+}$;*Klf5*$^{flox/flox}$ mice. These mice exhibited
200 necrotic fibers and infiltrating inflammatory cells, and an extensive area of regenerating
201 myofibers with prolonged expression of eMyHC (Figure 2B and C). Analysis of the
202 distribution of myofiber diameters revealed that *Klf5* deletion in SCs significantly
203 shifted regenerating myofibers towards smaller diameters (Figure 2D), suggesting
204 differentiation and/or maturation of muscle fibers were impaired by the loss of Klf5.

205 Twenty-eight days after CTX injury in control mice, muscle regeneration was
206 nearly complete, as evidenced by the presence of regenerated, mature fibers and

disappearance of inflammatory cells, as previous described (Ingalls et al., 1998). However, the regeneration process was retarded in the injured muscle of *Pax7*$^{CE/+}$;*Klf5*$^{flox/flox}$ mice, and massive deposition of collagen I, indicating enhanced fibrosis, was observed (Figure 2E). In addition, the regenerating myofibers were still shifted toward smaller diameters (Figure 2F). These results indicate that Klf5 is required for proper SC-mediated muscle regeneration after skeletal muscle injury.

Klf5 is required for myoblast differentiation

The molecular mechanism responsible for muscle regeneration mimics that for skeletal muscle differentiation, and the compromised muscle regeneration after SC-selective *Klf5* deletion suggested to us that Klf5 is necessary for proper skeletal muscle cell differentiation. To test that idea, we used C2C12 myoblasts, a widely-employed cell line that retains the potential to differentiate into myotubes. *Klf5* mRNA was induced after induction of C2C12 cells differentiation and reached a peak on day 4 of myoblast differentiation (Figure 3-figure supplement 1A). Klf5 protein was detected after 2 days of differentiation (Figure 3-figure supplement 1B) and was frequently colocalized with myogenin in the nuclei of differentiating myotubes, which is consistent with the pattern observed during myogenic differentiation of SCs (Figure 3-figure supplement 1B and Figure 1C).

To test the requirement for Klf5 in myoblast differentiation, we generated *Klf5*-null C2C12 cells using a CRISPR-Cas9 system (Ran et al., 2013). Three *Klf5*-null clones and three control clones were established (Figure 3- figure supplement 2A), and it was confirmed that both alleles were targeted by deletion and/or frame-shift mutation at the target loci in the *Klf5*-null clones (Figure 3-figure supplement 2B). Klf5 protein

231 was not detectable after induction of differentiation in any of the three *Klf5*-null clones
232 (Fig. 3A and Figure 3-figure supplement 2A), and myotube formation was significantly
233 impaired as compared to the control clones (Figure 3 and Figure 3-figure supplement
234 2A). This effect occurred concomitantly with decreased expression of myogenin and
235 MyHC on day 4 of differentiation (Figure 3A-C). To determine whether forced
236 expression of Klf5 could rescue the compromised differentiation of *Klf5*-null clones,
237 Klf5 was exogenously introduced using a retrovirus harboring murine Klf5 (RV-Klf5).
238 *Klf5*-null C2C12 cells transfected with RV-Klf5 successfully formed myotubes when
239 stimulated to differentiate, whereas *Klf5*-null cells infected with an empty retrovirus
240 failed to do so (Figure 3D). In addition, immunohistochemistry and western blotting
241 demonstrated that expression of MyHC and myogenin was partially rescued by the
242 forced expression of Klf5 (Figure 3D-F). Klf5 thus appears to be required for a
243 myoblast differentiation.

244 This requirement for Klf5 in myoblast differentiation was further confirmed by
245 knocking down *Klf5* using specific small interfering RNA (siRNA) in C2C12 cells.
246 Immunohistochemistry indicated that the *Klf5* knockdown efficiently inhibited the
247 induction of myogenin (Figure 3-figure supplement 3A and B). At the same time,
248 myotube formation was significantly impaired in the *Klf5* knockdown cells, as
249 quantified based on the Fusion index, which represents the fraction of MyHC-positive,
250 fused myotubes that contain at least three nuclei (Figure 3-figure supplement 3C and D).
251 Although previous reports have shown the involvement of Klf5 in controlling cell
252 proliferation in several cancer cell lines (Sun et al., 2001), *Klf5* knockdown did not
253 affect C2C12 cell proliferation (Figure 3- figure supplement 3E).

254 Because previous studies have shown cooperation and competition among Klf

members (Sunadome et al., 2011), we analyzed the effects of *Klf5* knockdown on expression of other Klf members. Levels of *Klf6*, *Klf13, Klf15*, and *Klf16* expression were modestly, but significantly, increased in *Klf5* knockdown cells on day 3 (Figure 3-figure supplement 1C). On the other hand, expression of *Klf10* and *Klf11* was decreased in *Klf5* knockdown cells.

Klf5 is required for induction of myogenesis-related genes

The observation that Klf5 is required for myoblast differentiation in both SCs and C2C12 cells led us to examine the consequences of *Klf5* knockdown on a genome-wide scale. A series of RNA-seq analyses of differentiating myoblasts and myotubes transfected with siRNA targeting Klf5 or control RNA were performed. In line with the suppressed myoblast differentiation, expression of a set of genes involved in myogenesis was significantly decreased in *Klf5* knockdown cells (Fig. 4A). Among the 12744 expressed transcripts (normalized counts >4), 1472 with RefSeq annotations were reduced by >1.5-fold on day 3 in the *Klf5* knockdown cells as compared to the control cells. Gene ontology analysis revealed that the genes whose expression was reduced by *Klf5* knockdown had significant enrichment of functional annotations for myogenesis and muscle cell development (Figure 4B). Among the 934 genes exhibiting a >1.5-fold increase in expression in *Klf5* knockdown cells, no gene sets directly related to myogenesis were significantly enriched as compared to control cells on day 3 (Figure 4-source data 1).

We next assessed the effects of *Klf5* knockdown on MyoD-regulated genes. Analysis of MyoD binding sites using previously reported MyoD ChIP sequencing (ChIP-seq) of C2C12 myotubes differentiated for 2 days (Cao et al., 2010) revealed that

among the Refseq genes, 753 that contained nearby sites bound by MyoD were upregulated by >2-fold on day 3 as compared with day 0. These genes are most likely direct MyoD targets and are highly enriched with myogenesis-related genes. The effect of *Klf5* knockdown on the expression of MyoD-regulated genes became more pronounced as the course of differentiation proceeded (Figure 4C), and expression of those MyoD-regulated genes on day 3 was significantly decreased by *Klf5* knockdown (Figure 4C and D). This distinct pattern of gene expression is exemplified by *Myog* and *Myl4* (Figure 4E). Quantitative PCR analysis confirmed that expression of MyoD-regulated genes, as exemplified by *Myog*, *Mybph*, *Myl4* and *Myom2*, was significantly decreased by *Klf5* knockdown in C2C12 cells on day 3 post-differentiation (Figure 4F). This indicates that Klf5 is required for expression of these MyoD-regulated genes. Remarkably, *de novo* motif analysis revealed that the top motifs in the MyoD-bound cistrome included ones closely matched with known consensus myogenin (E-box), Mef2 and Klf5 binding motifs, which suggests potential co-localization of MyoD, Mef2 and Klf5 at MyoD-regulated enhancers (Figure 4G). Cao et al. previously showed that the motif for Sp1 is enriched in regions bound by MyoD (Cao et al, 2010). The previously identified Sp1 motif contains a core 5'-CCGCCC-3' sequence, which matches a subset of the Klf motif ranked as 4th in our *de novo* motif analysis. This suggests the Sp1 motif may also be enriched. Indeed, enrichment analysis of a known Sp1 motif showed that the Sp1 motif is enriched in the MyoD binding regions (Figure 4G).

Klf5 regulates myogenesis-related genes in concert with MyoD and Mef2

The observation that the MyoD-bound cistrome was significantly enriched in the KLF5

303 motif led us to test the hypothesis Klf5 regulates genes involved in myogenesis in
304 concert with MyoD and Mef2. To investigate the location of Klf5 during the course of
305 myoblast differentiation, we performed ChIP-seq using a Klf5 specific antibody. In
306 addition, we used published ChIP-seq data to analyzed the binding sites of Mef2D in
307 C2C12 myotube on day 5, the major Mef2 isoform involved in expression of late
308 muscle-specific genes (Sebastian et al., 2013). As expected, Klf5 bound to the
309 regulatory regions of myogenesis-related genes, as exemplified by *Myog*, *Myod1*, *Myl4*
310 and *Mybph*, throughout the course of differentiation (Figure 5A and Fig 5-figure
311 supplement 1). MyoD and Mef2D binding was frequently observed at those gene loci.
312 The recruitment of Klf5, MyoD and Mef2 to the *Myog* enhancer was further confirmed
313 using ChIP-QPCR (Figure 5-figure supplement 2A-C).

314 Figure 5B shows a heatmap of Klf5, MyoD, and Mef2D binding around the top
315 1000 Klf5 binding peaks in C2C12 myotubes on day 5. Approximately half of the Klf5
316 peaks had significant MyoD binding peaks in close proximity. An association with
317 Mef2D was also observed in many Klf5 binding regions. Consistent with these findings,
318 genome-wide binding profiles showed that there is significant overlap among the Klf5,
319 MyoD and Mef2D cistromes (Figure 5C and 5D). Among 4382 Klf5 peaks observed on
320 day 5 post-differentiation, 757 loci (17.2%) were also bound by both MyoD and Mef2D,
321 and another 1467 sites (33.4%) were bound by either MyoD or Mef2D (Figure 5E).
322 Moreover, Klf5 binding to the MyoD and Mef2D binding peaks increased as
323 differentiation progressed (Figure 5C and 5D, compare day 0 vs. day 2 and 5).
324 Co-immunoprecipitation showed that Klf5 directly associated with MyoD and Mef2 *in*
325 *vitro* (Figure 5F). These results suggest that Klf5, MyoD and Mef2 work together to
326 drive expression of a set of genes involved in myogenic differentiation.

Only a small fraction of the regions that had Klf5 binding before differentiation (day 0) had significant MyoD binding in close proximity after starting differentiation into myotubes (Figure 5-figure supplement 3). This is in contrast to the Klf5-bound regions on day 5 (Figure 5B), which showed strong association with MyoD. The association of Klf5 with loci at which Klf5 was already bound before starting differentiation (day 0) was decreased or unchanged over the course of differentiation (Figure 5-figure supplement 3). This was in sharp contrast to the association of Klf5 recruited after starting myogenic differentiation (Figure 5B). Collectively then, a majority of regions that increasingly acquire Klf5 binding during differentiation are also bound by MyoD in proximity to the Klf5 within myotubes. On the other hand, at many observed Klf5 binding regions in myoblasts, binding is decreased during differentiation and not associated with MyoD binding within myotubes. These results suggest that Klf5 has different targets and functions in myoblasts vs. myotubes. Because this study focuses on Klf5's function during muscle differentiation and regeneration, we will characterize Klf5 binding mainly in myotubes.

Analysis of Klf5-bound motifs revealed that the top motif among the Klf5 cistrome matches the consensus of Krüppel-like factor (Figure 5G). The Myf5 (E-box consensus bound by MRF, including MyoD) and Mef2D motifs were also identified in the *de novo* motif analysis, suggesting that colocalization of Klf5, MyoD and Mef2 are programmed by cis-regulatory logic. These results demonstrate a significant role for Klf5 in myogenic differentiation, acting in coordination with two other myogenic transcription factors, MyoD and Mef2.

To assess the functional significance of Klf5 in the regulation of muscle-specific target genes, we performed luciferase assays (Figure 5H). To eliminate effects of

endogenous MyoD and MEF2D expression, HEK293T cells were co-transfected with Klf5, MyoD, MEF2D and *Myog* promoter-luciferase plasmids, which contained the proximal promoter region bound by Klf5, MyoD and Mef2 determined from each ChIP-seq (Figure 5B). We found that Klf5 alone activated the *Myog* reporter. Moreover, Klf5, MyoD and MEF2D activated the *Myog* reporter additively (Figure 5H). Together, these findings indicate that Klf5 is an active transcription factor for myogenesis, cooperating with MyoD and Mef2.

Klf5 is necessary for the recruitment of MyoD to muscle-specific target genes

Our results indicate that the Klf5 cistrome significantly overlaps those of MyoD and Mef2 (Figure 5A-E), and Klf5 directly interacts with MyoD and Mef2 (Figure 5F). In addition, the compromised myogenic phenotype observed in *Klf5* knockout SCs and C2C12 cells (Figures 2-4), and the reduction in the fraction of MyoD-regulated gene expression induced by *Klf5* knockdown in differentiating C2C12 cells (Figure 4C, D), also suggest Klf5 affects MyoD-dependent gene regulation. To test whether Klf5 is required for recruitment of MyoD to target sites, we performed ChIP-seq of MyoD in *Klf5*-null and GFP-targeted control C2C12 myotubes to determine the effects of the *Klf5* deletion on the MyoD cistrome. Although levels of MyoD and MEF2 protein were not affected by *Klf5* deletion (Figure 6- figure supplement 1), ChIP-seq revealed that MyoD binding was markedly decreased in *Klf5* knockout cells compared to the GFP-targeted control cells on 3 day post-differentiation, as exemplified with *Myod1*, *Myog*, *Myl4* and *Mybph* (Figure 6A and 6B). This decrease in MyoD binding after *Klf5* deletion was similarly observed in another set of MyoD ChIP-seqs performed independently (Figure 6- figure supplement 2). The impaired recruitment of MyoD to the regulatory region of

375 myogenic genes was further confirmed by ChIP-qPCR (Figure 6C). These results
376 suggest that Klf5 plays a significant role in the recruitment of MyoD to target genes.
377
378 **Klf5 is required for satellite cell differentiation**
379 To further test the requirement for Klf5 in SC differentiation, SCs were isolated from
380 the EDL muscle of *Pax7*$^{CE/+}$;*Klf5*$^{flox/flox}$ and control mice. Those SCs were cultured in
381 growth medium for 3 days, then treated with 4OH-Tmx for 2 days to induce *Klf5*
382 deletion by Cre-ER. In 4OH-Tmx treated *Pax7*$^{CE/+}$;*Klf5*$^{flox/flox}$ SCs, Klf5 protein was
383 undetectable. In these Klf5 knockout cells, myogenin protein was markedly reduced as
384 compared to that in control *Pax7*$^{CE/+}$;*Klf5*$^{flox/flox}$ SCs without 4OH-Tmx treatment
385 (Figure 7A). In addition, mRNA expression levels of *Klf5* target genes exemplified by
386 *Myog*, *Mybph* and *Myom2* were significantly decreased in those cells (Figure 7B).
387 Collectively, these results indicate that Klf5 is indispensable for differentiation of
388 primary SCs as well as C2C12 cells.
389

Discussion

Several pieces of evidence gathered in this study clarify the essential role of Klf5 in the control of adult skeletal muscle regeneration. First, although expression of Klf5 protein remained low in $Pax7^{+}$ quiescent and activated SCs, Klf5 was significantly induced in myoblasts differentiating after skeletal muscle injury (Fig. 1). Second, SC-specific deletion of *Klf5* markedly impaired muscle regeneration after injury due to a failure of differentiation (Fig. 2), which confirmed the pivotal involvement of Klf5 in muscle regeneration *in vivo*. Third, suppressed differentiation into myotubes was observed in *Klf5*-null C2C12 myoblasts (Fig. 3), after specific *Klf5* knockdown *in vitro* (Figure 3-figure supplement 3) and SCs from Klf5 KO mice (Fig. 7). Fourth, inhibition of Klf5 affected transcriptional regulation of muscle-related genes by MRFs, including MyoD and myogenin (Figs. 4-6). Collectively, these observations indicate that Klf5 is an essential component of the transcriptional regulatory network governing muscle differentiation and regeneration.

The molecular mechanism underlying muscle regeneration recapitulates many aspects of the process of muscle development. In particular, many of the transcription factors that control embryonic myogenesis also contribute to adult regenerative myogenesis. When a muscle is injured, hepatocyte growth factor (HGF), released from the basal lamina of the injured muscle triggers SC activation (Tatsumi et al., 1998). The activated SCs migrate and rapidly proliferate to give rise to $Pax7^{+}Myf5^{+}$ cells, which activate the MRF cascade (Cooper et al., 1999; Kuang et al., 2007). Our present results indicate that Klf5 is induced in myoblast-committed, non-dividing $Pax7^{low}MyoD^{+}$ SCs after they are triggered to differentiate into myocytes. Likewise, *Klf5* mRNA remained low in C2C12 myoblasts and SCs cultured in growth media. *Klf5* is greatly upregulated

414 only after switching to differentiation media (Fig. 1C, Figure 3- figure supplement
415 1A-B). In differentiating myoblasts Klf5 is required for expression of *Myog* and
416 muscle-specific genes. Given that Klf5 enhances binding of MyoD to its target sites,
417 these findings collectively suggest that Klf5 is an important regulator that links the early
418 specification program driven by MyoD and Myf5 to the late myotube formation and
419 maturation program driven by myogenin and Mrf4.

420 To further elucidate the regulatory function of Klf5 in myogenesis, it will be
421 important to determine how Klf5 expression is induced during myocyte differentiation
422 and regeneration. Klf5 is reportedly induced in response to external/endogenous stimuli
423 through various signaling cascades, including p38MAPK (Nandan et al., 2004; Oishi et
424 al., 2010), ERK1/2 (Kawai-Kowase et al., 1999) and IL-1β/HIF-1α (Mori et al., 2009).
425 We previously showed that the p38MAPK pathway controls upregulation of Klf5 in
426 response to angiotensin II in smooth muscle cells (Oishi et al., 2010). The p38MAPK
427 pathway is activated immediately after the onset of myogenic differentiation and muscle
428 regeneration (Chen et al., 2007), and is essential for myoblast differentiation (Gonzalez
429 et al., 2004). Moreover, genome-wide transcriptome analysis of SCs with
430 muscle-specific p38α deletion or C2C12 cells treated with a p38 MAPK inhibitor
431 revealed that p38α is responsible for induction of Klf5 during myoblast differentiation
432 (Segales et al., 2016). Interestingly, that study also showed that inhibiting p38 signaling
433 does not affect expression of MyoD. It therefore seems likely that Klf5 is an essential
434 component of the transcriptional machinery activated by p38 MAPK during myogenic
435 differentiation. A previous study showed that Klf2 and Klf4 are induced by ERK5
436 signaling and contribute to muscle cell fusion (Sunadome et al., 2011). Microarray
437 analyses in that study indicate that Klf5 expression is not affected by inhibition of

ERK5 signaling (GSE25827). This is in agreement with our previous observations that Klf5 expression was unaffected by a MEK inhibitor in smooth muscle cells (Oishi et al., 2010). These findings indicate that members of Krüppel-like factor family differentially contribute to different processes during muscle differentiation and maturation. That said, it is possible that the loss of Klf5 is compensated by other Klf members, as we observed modest changes in the expression of other Klfs in Klf5-deficient C2C12 cells (Figure 3-figure supplement 1). Future studies of possible cooperation and competition among Klf members will be important for elucidating their functional roles in muscle biology. In addition, we found that exogenous Klf5 increased the level of eMyHC in Klf5-deleted C2C12 myotubes, but did not fully recapitulate the normal level of eMyHC expression (Figure 3). This insufficient rescue may reflect differences between endogenous and exogenous Klf5, including the levels and timing of Klf5 expression. In the control cells, for example, Klf5 was transiently upregulated early during differentiation, but this temporal regulation of Klf5 was lost in cells in which exogenous Klf5 was stably expressed. Future studies will also need to address the temporal regulation of Klf members during muscle differentiation and regeneration.

Our ChIP-seq results indicate that deletion of Klf5 impairs recruitment of MyoD. This demonstrates that Klf5 is required for formation of MyoD-containing transcriptional regulatory complexes in at least a subset of the MyoD cistrome (Fig. 6). Recent studies have identified several transcription factors that interact with MyoD. For instance, Runx1 is induced in response to muscle injury and acts cooperatively with MyoD and c-Jun to regulate muscle regeneration (Umansky et al., 2015). TEAD4 is another factor reportedly recruited and bound to the locus also occupied by MyoD during the course of myogenic differentiation (Benhaddou et al., 2012). Inhibition of

462 Runx1 or TEAD4 suppresses myogenic differentiation and regeneration, suggesting
463 those two transcription factors, together with MyoD, are necessary to drive muscle
464 regeneration. Of interest, we observed the sequence motif bound by Runx to rank 4th
465 and the MCAT motif bound by TEAD4 to rank 6th among the *de novo* motifs identified
466 in regions bound by Klf5 in myotubes differentiated for 5 days (Fig. 5F and data not
467 shown). These data suggest that Klf5 promotes myogenic differentiation by interacting
468 with multiple transcription factors, including MyoD, Mef2, Runx1 and TEAD4. It is
469 likely these transcription factors are differentially regulated in response to different
470 environmental cues and/or endogenous signaling. Accordingly, the interplay between
471 these multiple factors would enable spatiotemporal regulation and fine tuning of
472 muscle-related gene expression. It would be important to further clarify the logic of
473 transcriptional regulation by these multiple transcription factors. It would also be worth
474 noting that there appears to be a complex cross-regulation of the expression of these
475 factors. For instance, in addition to myogenin, Klf5 appears to regulate TEAD4 because
476 there were Klf5 binding peaks in the vicinity of the genes in our ChIP-seq, and *Klf5*
477 knockdown reduced TEAD4 levels (data not shown). In addition, based on a published
478 microarray analysis of effects of an individual MEF2 isoform (GSE63798) (Estrella et
479 al., 2015) and our results from smooth muscle cells (Oishi et al., 2010), it appears Klf5
480 is regulated by MEF2A. This reciprocal regulation of Klf5 and other myogenic
481 transcription factors support the notion that Klf5 is a component of an intricate
482 transcription factor network that regulates muscle differentiation and regeneration.

483 In addition to MyoD and Mef2 identified in the present study, Klf5 has been
484 shown to interact with various other transcription factors and cofactors. For instance we
485 showed that Klf5 interacts with C/EBBβ and δ to regulate adipocyte differentiation

(Oishi et al., 2005), interacts with PPARδ to regulate lipid metabolic genes (Oishi et al., 2008), and interacts with C/EBPα to control the response to renal injury (Fujiu et al., 2011). Klf5 also interacts with unliganded RAR/RXR to induce phenotypic modulation of vascular smooth muscle cells (Fujiu et al., 2005). By taking advantage of this mechanism, we showed that an RAR agonist can inhibit induction of Klf5 target genes, thereby suppressing smooth muscle cell proliferation and neointima formation. We may therefore be able to manipulate the muscle regeneration program by altering the activity of Klf5 through its interacting partners. In sum, our results provide evidence that during skeletal muscle regeneration and myoblast differentiation, Klf5 regulates the expression of late muscle-specific genes in concert with MyoD and Mef2. This finding suggests that it will be of interest to investigate this pathway further with respect to the control of muscle regeneration. It would also be interesting to know whether Klf5-mediated pathways are involved in such pathological conditions as sarcopenia.

Materials and Methods

Mice

Klf5$^{flox/flox}$ mice (Takeda et al., 2010) were crossed with *Pax7*$^{CreERT2/+}$ mice (Abbreviated *Pax7*$^{CE/+}$ (Lepper et al., 2009)) to generate *Pax7*$^{CE/+}$;*Klf5*$^{flox/flox}$ mice. All mice used in this study had a C57BL/6J genetic background, were between 8-12 weeks old and had age-matched littermate controls. Animal experimentation was approved by the Experimental Animal Care and Use Committee of Tokyo Medical and Dental University (approval numbers 2013-027C12 and 0170280C) .

Muscle regeneration

Tamoxifen (Sigma-Aldrich, St. Louis, MO) was dissolved in corn oil (Nakarai, Tokyo, Japan) to a concentration of 20 mg/ml. Eight- to twelve-week-old *Klf5*$^{flox/flox}$ and *Pax7*$^{CE/+}$;*Klf5*$^{flox/flox}$ mice were intraperitoneally injected with 100 µl of tamoxifen solution daily for 5 days prior to induction of muscle injury. To induce muscle regeneration, 100 µl of 10 mM cardiotoxin (CTX: Sigma-Aldrich) were injected intramuscularly into the tibialis anterior (TA) muscle of anesthetized mice using a 29G syringe. Regenerating muscles were isolated 4, 7 and 28 days after CTX injection, immediately frozen in cooled isopentane in liquid nitrogen, and stored at -80˚C before being cryosectioned. To analyze the distribution of fiber diameters, at least three sections from each of four *Pax7*$^{CE/+}$;*Klf5*$^{flox/flox}$ mice and four *Pax7*$^{+/+}$;*Klf5*$^{flox/flox}$ (control) mice were examined. Immunofluorescent images of laminin were acquired, after which the area surrounded by the laminin signal in each cross-section was quantified using Olympus cellSense Digital Imaging software. In each mouse, the

524 diameters of 1000 (for CTX day 7) or 500 (for CTX day 28) regenerating fibers that had
525 centrally located myonuclei were determined.
526
527 **Satellite cell isolation, culture conditions and transfection**
528 Extensor digitorum longus (EDL) muscles were isolated from wild type C57/BL6 males
529 and digested in type I collagenase (Worthington Biochemical Corp., Freehold, NJ). SCs
530 were obtained from isolated myofibers by trypsinization in 0.125% trypsin-EDTA
531 solution for 10 min at 37˚C with 5% CO_2. SCs were cultured in GlutaMax DMEM (Life
532 Technologies, Grand Island, NY) supplemented with 20% fetal bovine serum (FBS:
533 Hyclone, Thermo scientific, Hudson, NH), 1% chick embryo extract (US Biological,
534 Salem, MA), 10 ng/ml basic fibroblast growth factor (Cell Signaling Technology,
535 Beverly, MA), and 1% penicillin-streptomycin at 37˚C with 5% CO_2. Myogenic
536 differentiation was induced in GlutaMax DMEM supplemented with 2% horse serum
537 and 1% penicillin-streptomycin at 37˚C with 5% CO_2.
538 To assess satellite cells obtained from $Pax7^{CE/+};Klf5^{flox/flox}$ mice, the cells were
539 treated with 1 μM 4-hydroxytamoxifen (4OH-Tmx; Sigma-Aldrich, H7904) or vehicle 3
540 days after isolation, then grown in growth medium for another 2 days.
541 C2C12 mouse myoblasts (RRID:CVCL_0188) were purchased from the ATCC
542 (ATCC® #CRL-1772, passage number 6-8, Rockville, MD) . The identity was not
543 authenticated by our hands. Cells were free from mycoplasma contamination confirmed
544 by monthly tests for mycoplasma. Cells were cultured in DMEM (Nakarai) containing
545 10% FBS and 1% penicillin-streptomycin at sub-confluent densities. C2C12 cells were
546 differentiated into myotubes by replacing growth medium with medium containing 2%
547 horse serum with antibiotics (differentiation medium, DM). To knock down Klf5 in

548 C2C12 cells, siKlf5 (Thermo scientific, Dharmacon, siRNA-SMARTpool,
549 M-062477-01-0005) treatment was carried out using RNAiMAX (Life Technologies)
550 according to the manufacturer's instructions. Each experiments were biologically
551 replicated at least three times.
552
553 **Generation of *Klf5* knockout C2C12 cells**
554 *Klf5* gene was engineered as described previously (Ran et al., 2013). Briefly, a plasmid
555 vector containing clustered regularly interspaced short palindromic repeats
556 (CRISPR)-Cas9 endonuclease coupled with paired guide RNAs flanking the mouse *Klf5*
557 gene was transiently transfected into C2C12 cells. Deletion of targeted loci was
558 confirmed by sequencing. Cells transfected with a plasmid vector carrying
559 CRISPR-Cas9 endonuclease coupled with paired guide RNAs flanking the GFP
560 sequence were used as a control (Abbreviated GFP-targeted control).
561
562 **Immunofluorescent Staining**
563 Cryosections (10 μm thickness) were fixed in 4% paraformaldehyde (PFA)/PBS for 10
564 min at room temperature. For antigen retrieval, the sections were incubated in 0.01 M
565 citric acid solution (pH 6.0) for 10 min at 80˚C. The sections were then permeabilized in
566 methanol for 6 min at -20˚C. Cultured cells were also fixed in 4% PFA/PBS for 10 min
567 at room temperature and permeabilized in 0.5% TritonX-100/PBS solution for 5 min at
568 room temperature after washing 3 times. The sections and cells were then blocked in
569 5% BSA/PBS blocking solution, after which primary antibodies prepared in blocking
570 solution were added and incubated at 4˚C overnight. This was followed by 3 washes in
571 PBS and incubation with Alexa fluor-conjugated antibodies (Life Technologies) in

572 blocking solution for 1 h at room temperature. After another 3 washes in PBS, the
573 sections were counterstained with Hoechst 33342 solution at room temperature for 3
574 min. The slides were mounted with a coverslip and Fluoromount-G (SouthernBiotech,
575 Birmingham, AL). Immunofluorescent signals from stained sections and cells were
576 captured using a LSM710 confocal imaging system (Carl Zeiss, Inc., Oberkochen,
577 Germany) or OLYMPUS IX73 fluorescence inverted fluorescence microscope with an
578 Olympus DP80 camera and Olympus cellSense Digital Imaging software (Tokyo,
579 Japan).
580
581 **Retroviral Infection and Plasmid Vectors**
582 Murine *Klf5* cDNA was cloned into the retroviral backbone pMX-GFP (Cell Biolabs,
583 San Diego, CA) to produce pMX-Klf5-GFP (RV-Klf5), after which the retroviruses
584 were packaged into the Platinum-E (PLAT-E) Retroviral Packaging Cell Line (Cell
585 Biolabs) according to the manufacturer's instructions. Retroviral infection was
586 accomplished at 37˚C overnight using PLAT-E supernatant supplemented with 4 μg/ml
587 polybrene.
588
589 **Immunoprecipitation**
590 Cellular protein (100 μg) from differentiated C2C12 myotubes was mixed with 2 μg of
591 anti-MyoD, anti-Klf5 or anti-MEF2 antibody and incubated overnight at 4˚C. Twenty μl
592 of protein G Dynabeads (1001D; Life Technologies) were then added to each sample
593 and incubated for 1 h at 4˚C. After the incubation, the samples were washed 6 times
594 with wash buffer (10 mM Tris-HCl, 100 mM NaCl, 1 mM EDAT, 1 mM DTT, 0.5%
595 NP40 and 0.5% TritonX-100), resuspended in SDS sample buffer and heated at 98˚C for

5 min prior to electrophoresis. Each experiments were biologically replicated at least three times.

Immunoblotting

Proteins were quantified using a BCA Protein assay kit (Pierce, Rockford, IL) following the manufacturer's protocol. Thirty μg of total protein were separated by 10% SDS-PAGE and transferred onto PVDF Immobilon-P membranes (Millipore, Billerica, MA). Western blotting was performed using ECL Prime detection reagent (GE, Waukesha, WI) according to the manufacturer's instructions. Each experiments were biologically replicated at least three times.

Real-time PCR analysis

Total RNA was isolated from cultured cells using an RNeasy Mini Kit (Qiagen, Valencia, CA) according to the manufacturer's protocol. RNA or ChIP-DNA were analyzed using real-time PCR with a KAPA SYBR Fast qPCR Kit (Kapa Biosystems, Woburn, MA). The primers for qPCR are listed in Table2. Each experiments were biologically replicated at least three times.

Luciferase assay

Murine *Klf5* (Genbank accession number: NM_009769) was sub-cloned into p3xFlag-CMV-7.1 vector. The Myog-Luciferase vector was kindly provided by Dr. T. Sato (Kyoto Prefectural University of Medicine, unpublished). The *Myod1* expression vector was a gift of Dr. P. Maire (Institute Cochin) (Santolini et al., 2016). The *Mef2d* expression vector was kindly provided by Dr. E. Olson (University of Texas

Southwestern Medical Center). The 293T cells were transfected with a CMV-Renilla luciferase control reporter plasmid along with Myog-Luciferase, *Klf5*, *Myod1* and *Mef2d* expression plasmids. The total amount of plasmid DNA was kept constant using p3xFlag-CMV-7.1 empty vector. Forty-eight hours after transfection, the cells were lysed in Passive Lysis Buffer (Promega) and shaken for 15 min. The lysates were used for measurement of firefly and Renilla luciferase activities using EnSpire (PerkinElmer, Waltham, MA, USA), after which the firefly luciferase activity was normalized to the Renilla luciferase activity.

Library preparation and RNA-seq

PolyA-tagged RNA was pulled down from total RNA using oligo-dT magnetic beads. RNA-seq libraries were multiplexed and prepared according to the manufacturer's protocol (NEB cat#E7530, Ipswich, MA). Libraries were paired-end sequenced on a HiSeq2500 sequencer (Illumina, San Diego, CA). Reads were aligned to the mm9 genome using the default parameter for RNA-star. Aligned read files were analyzed with HOMER (http://homer.salk.edu/homer/) to calculate RPKM from the gene bodies of RefSeq genes and perform motif analysis. Reads counts were normalized using DESeq2 (Love et al., 2014).

Chromatin Immunoprecipitation (ChIP)

Undifferentiated C2C12 myoblasts and myotubes differentiated for 2 or 5 days were used for Klf5 ChIP. For MyoD ChIP in CRISPR-engineered cells, cells differentiated for 3 days were used. Cells were fixed in 1% formaldehyde for 10 min at room temperature. The reactions were stopped by adding glycine to a final concentration of

644 0.125 M and incubating for 10 min at room temperature. After washing with PBS, the
645 cell pellet was lysed in ice-cold Cell Lysis Buffer, incubated on ice for 10-20 min and
646 centrifuged at 3000 rpm for 5 min at 4°C. The pellet was further lysed in ice-cold RIPA
647 buffer and incubated on ice for 10 min. The resultant cell lysate was sonicated using an
648 ultrasonicator (output 50, 30-s pulses then 1-min pause × 13 times; UD-100: TOMY
649 Seiko, Tokyo, Japan). The chromatin was then pre-cleared by incubating with
650 Sepharose® CL-4B (Sigma- Aldrich) for 2 h at 4°C with constant rotation. After
651 centrifugation, anti-MyoD or anti-Klf5 antibody was added and rotated overnight at 4°C.
652 Protein A-Sepharose® 4B fast flow (BD) was then added and incubated for 1 h at 4°C
653 with constant rotation. Thereafter, the beads were washed 4 times with RIPA buffer, 6
654 times with LiCl buffer and 3 times with TE buffer, then eluted with 2% SDS solution.
655 After reverse cross-linking at 65°C overnight, the chromatin immunoprecipitate and
656 Input were treated with RNase (37°C, 1 h) and Proteinase K (42°C, 1 h). The recovered
657 chromatin was purified using a MiniElute PCR Purification kit (Qiagen) and used for
658 real-time PCR analysis.
659
660 **Library preparation and ChIP-Seq**
661 Sequencing libraries were prepared from collected DNA by using NEB next Ultra DNA
662 library prep kit for Illumina according to the manufacturer's protocol (NEB, Ipswich,
663 MA). Libraries were PCR-amplified for 12-15 cycles, size selected by gel extraction
664 and sequenced on a Hi-Seq 1500 (Illumina) for 51 cycles.
665
666 **ChIP-seq analysis**
667 ChIP-seq data for MyoD and Mef2D binding in C2C12 cells (SRA010854 and

SRP017715) were downloaded from NCBI. Reads were mapped to the mm9 genome using STAR (Dobin et al., 2013). Peak calling and annotation was performed using HOMER version 4 (Heinz et al., 2010) for MyoD and Klf5, and using MACS2 (Zhang et al., 2008) for Mef2D. Peaks that overlapped blacklisted regions (Consortium, 2012) or simple repeat regions were removed. Homer-identified MyoD and Klf5 peaks with scores ≥20 were considered high confidence binding sites and used for further analyses, except for detection of MyoD peaks in the vicinity of Klf5 peaks in Figure 5. To make a set of potential MyoD-regulated genes, RefSeq genes that contained MyoD peaks within a region -1500 bp from TSS to +1500 bp from TTS were first chosen. Then genes whose normalized counts were increased ≥2-fold in C2C12 myotubes relative to those in myoblasts were selected. The resultant MyoD target gene set contained 753 RefSeq genes. This gene set was highly enriched in GO terms related to muscle differentiation. All RNA-seq and ChIP-seq data are available in the GEO under the accession number GSE80812. To identify enriched motifs in ChIP-seq peaks, we used Homer's findMotifsGenome.pl software (Heinz et al., 2010).

Statistical Analysis

Sample sizes were not based on power calculations. No animals were excluded from analyses. Comparisons between two groups were analyzed using two-tailed Student's *t*-test. Differences among more than two groups were analyzed using one-way ANOVA followed by Tukey-Kramer post-hoc tests. Values of $p < 0.05$ were considered statistically significant, except in analyses involving RNA-seq and ChIP-seq. All data are means ± SEM.

692 **Additional Information**

693 Details of antibodies and sequences for qPCR are described in Tables 1 and 2.

694

Acknowledgement

We are grateful to Dr. A. Aiba (The University of Tokyo) and Dr. Y. Nakayama for providing pSpCas9 plasmid, Dr. P. Maire and Dr. I. Sakakibara for providing Myod1 expression plasmid, and Dr. T. Sato for providing Myog-Luciferase plasmid. We thank Dr. M. Kanagawa and Dr. S. Fukada for the technical advice for *Pax7*$^{CreERT2/+}$ mice and Dr. S. Takeda and Dr. N. Ito for the technical advice for SC culture. We thank Mrs. N. Yamanaka and Mrs. M. Hayashi for their excellent technical assistance (The University of Tokyo). We thank our colleagues in the Oishi Lab and members of the Manabe Lab for discussion.

This work was supported in part by JSPS KAKENHI Grant Number 26882020 (Grant-in-Aid for Research Activity Start-up to SH), 25H10 (to YO), and 15H01506 (to IM); AMED-CREST (to IM); and the grants from Nakatomi Health Science Foundation and the Uehara Memorial Foundation (to SH).

Author Contributions

S.H. directed and developed the project, performed most of the experiments, data analysis and wrote the manuscript. Y.O. developed and supervised the project, designed experiments, performed data analysis and wrote the manuscript. I.M. and F.R. contributed to data analysis and wrote the manuscript. Y.S. contributed to the *in vitro* studies, ChIP-qPCR and reviewed the manuscript.

References

Adam, P.J., Regan, C.P., Hautmann, M.B., and Owens, G.K. (2000). Positive- and negative-acting Kruppel-like transcription factors bind a transforming growth factor beta control element required for expression of the smooth muscle cell differentiation marker SM22alpha in vivo. J Biol Chem *275*, 37798-37806.

Benhaddou, A., Keime, C., Ye, T., Morlon, A., Michel, I., Jost, B., Mengus, G., and Davidson, I. (2012). Transcription factor TEAD4 regulates expression of myogenin and the unfolded protein response genes during C2C12 cell differentiation. Cell Death Differ *19*, 220-231.

Bieker, J.J. (2001). Kruppel-like factors: three fingers in many pies. J Biol Chem *276*, 34355-34358.

Buckingham, M., and Rigby, P.W. (2014). Gene regulatory networks and transcriptional mechanisms that control myogenesis. Dev Cell *28*, 225-238.

Cao, Y., Yao, Z., Sarkar, D., Lawrence, M., Sanchez, G.J., Parker, M.H., MacQuarrie, K.L., Davison, J., Morgan, M.T., Ruzzo, W.L., *et al.* (2010). Genome-wide MyoD binding in skeletal muscle cells: a potential for broad cellular reprogramming. Dev Cell *18*, 662-674.

Chanchevalap, S., Nandan, M.O., Merlin, D., and Yang, V.W. (2004). All-trans retinoic

740 acid inhibits proliferation of intestinal epithelial cells by inhibiting expression of the
741 gene encoding Kruppel-like factor 5. FEBS Lett *578*, 99-105.
742
743 Chen, S.E., Jin, B., and Li, Y.P. (2007). TNF-alpha regulates myogenesis and muscle
744 regeneration by activating p38 MAPK. Am J Physiol Cell Physiol *292*, C1660-1671.
745
746 Comai, G., and Tajbakhsh, S. (2014). Molecular and cellular regulation of skeletal
747 myogenesis. Curr Top Dev Biol *110*, 1-73.
748
749 Consortium, E.P. (2012). An integrated encyclopedia of DNA elements in the human
750 genome. Nature *489*, 57-74.
751
752 Cooper, R.N., Tajbakhsh, S., Mouly, V., Cossu, G., Buckingham, M., and Butler-Browne,
753 G.S. (1999). In vivo satellite cell activation via Myf5 and MyoD in regenerating mouse
754 skeletal muscle. J Cell Sci *112 (Pt 17)*, 2895-2901.
755
756 Dionyssiou, M.G., Salma, J., Bevzyuk, M., Wales, S., Zakharyan, L. and McDermott,
757 J.C. (2013). Krüppel-like factor 6 (KLF6) promotes cell proliferation in skeletal
758 myoblasts in response to TGFβ/Smad3 signaling. Skeletal Muscle *3*, 7.
759
760 Dobin, A., Davis, C.A., Schlesinger, F., Drenkow, J., Zaleski, C., Jha, S., Batut, P.,
761 Chaisson, M., and Gingeras, T.R. (2013). STAR: ultrafast universal RNA-seq aligner.
762 Bioinformatics *29*, 15-21.
763

764 Ema, M., Mori, D., Niwa, H., Hasegawa, Y., Yamanaka, Y., Hitoshi, S., Mimura, J.,
765 Kawabe, Y., Hosoya, T., Morita, M., *et al.* (2008). Kruppel-like factor 5 is essential for
766 blastocyst development and the normal self-renewal of mouse ESCs. Cell Stem Cell *3*,
767 555-567.
768
769 Estrella, N.L., Desjardins, C.A., Nocco, S.E., Clark, A.L., Maksimenko, Y., and Naya,
770 F.J. (2015). MEF2 transcription factors regulate distinct gene programs in mammalian
771 skeletal muscle differentiation. J Biol Chem *290*, 1256-1268.
772
773 Fong, A.P., and Tapscott, S.J. (2013). Skeletal muscle programming and
774 re-programming. Curr Opin Genet Dev *23*, 568-573.
775
776 Fujiu, K., Manabe, I., Ishihara, A., Oishi, Y., Iwata, H., Nishimura, G., Shindo, T.,
777 Maemura, K., Kagechika, H., Shudo, K., *et al.* (2005). Synthetic retinoid Am80
778 suppresses smooth muscle phenotypic modulation and in-stent neointima formation by
779 inhibiting KLF5. Circ Res *97*, 1132-1141.
780
781 Fujiu, K., Manabe, I., and Nagai, R. (2011). Renal collecting duct epithelial cells
782 regulate inflammation in tubulointerstitial damage in mice. J Clin Invest *121*,
783 3425-3441.
784
785 Gonzalez, I., Tripathi, G., Carter, E.J., Cobb, L.J., Salih, D.A., Lovett, F.A., Holding, C.,
786 and Pell, J.M. (2004). Akt2, a novel functional link between p38 mitogen-activated
787 protein kinase and phosphatidylinositol 3-kinase pathways in myogenesis. Mol Cell

Biol *24*, 3607-3622.

Gray, S., Wang, B., Orihuela, Y., Hong, E.G., Fisch, S., Haldar, S., Cline, G.W., Kim, J.K., Peroni, O.D., Kahn, B,B and Jain, M.K. (2007). Regulation of gluconeogenesis by Krüppel-like factor 15. Cell Metab *5*, 305-312.

Haldar, S.M., Jeyaraj, D., Anand, P., Zhu, H., Lu, Y., Prosdocimo, D.A., Eapen, B., Kawanami, D., Okutsu, M., Brotto, L., Fujioka, H., Kerner, J., Rosca, M.G., McGuinness, O.P., Snow, R.J., Russell, A.P., Gerber, A.N., Bai, X., Yan, Z., Nosek, T.M., Brotto, M., Hoppel, C.L. and Jain M.K. (2012). Kruppel-like factor 15 regulates skeletal muscle lipid flux and exercise adaptation. Proc Natl Acad Sci U S A *109*, 6739-6744.

Himeda, C.L., Ranish, J.A., Pearson, R.C., Crossley, M. and Hauschka, S.D. (2010). KLF3 regulates muscle-specific gene expression and synergizes with serum response factor on KLF binding sites. Mol Cell Biol *30*, 3430-3643.

Heinz, S., Benner, C., Spann, N., Bertolino, E., Lin, Y.C., Laslo, P., Cheng, J.X., Murre, C., Singh, H., and Glass, C.K. (2010). Simple combinations of lineage-determining transcription factors prime cis-regulatory elements required for macrophage and B cell identities. Mol Cell *38*, 576-589.

Ingalls, C.P., Warren, G.L., and Armstrong, R.B. (1998). Dissociation of force production from MHC and actin contents in muscles injured by eccentric contractions. J Muscle Res Cell Motil *19*, 215-224.

812

813 Kawai-Kowase, K., Kurabayashi, M., Hoshino, Y., Ohyama, Y., and Nagai, R. (1999).
814 Transcriptional activation of the zinc finger transcription factor BTEB2 gene by Egr-1
815 through mitogen-activated protein kinase pathways in vascular smooth muscle cells.
816 Circ Res *85*, 787-795.

817

818 Kuang, S., Kuroda, K., Le Grand, F., and Rudnicki, M.A. (2007). Asymmetric
819 self-renewal and commitment of satellite stem cells in muscle. Cell *129*, 999-1010.

820

821 Lepper, C., Conway, S.J., and Fan, C.M. (2009). Adult satellite cells and embryonic
822 muscle progenitors have distinct genetic requirements. Nature *460*, 627-631.

823

824 Lepper, C., Partridge, T.A., and Fan, C.M. (2011). An absolute requirement for
825 Pax7-positive satellite cells in acute injury-induced skeletal muscle regeneration.
826 Development *138*, 3639-3646.

827

828 Love, M.I., Huber, W., and Anders, S. (2014). Moderated estimation of fold change and
829 dispersion for RNA-seq data with DESeq2. Genome Biol *15*, 550.

830

831 Molkentin, J.D., and Olson, E.N. (1996). Combinatorial control of muscle development
832 by basic helix-loop-helix and MADS-box transcription factors. Proc Natl Acad Sci U S
833 A *93*, 9366-9373.

834

835 Mori, A., Moser, C., Lang, S.A., Hackl, C., Gottfried, E., Kreutz, M., Schlitt, H.J.,

836 Geissler, E.K., and Stoeltzing, O. (2009). Up-regulation of Kruppel-like factor 5 in
837 pancreatic cancer is promoted by interleukin-1beta signaling and hypoxia-inducible
838 factor-1alpha. Mol Cancer Res *7*, 1390-1398.
839
840 Nandan, M.O., Yoon, H.S., Zhao, W., Ouko, L.A., Chanchevalap, S., and Yang, V.W.
841 (2004). Kruppel-like factor 5 mediates the transforming activity of oncogenic H-Ras.
842 Oncogene *23*, 3404-3413.
843
844 Oishi, Y., Manabe, I., Imai, Y., Hara, K., Horikoshi, M., Fujiu, K., Tanaka, T., Aizawa,
845 T., Kadowaki, T., and Nagai, R. (2010). Regulatory polymorphism in transcription
846 factor KLF5 at the MEF2 element alters the response to angiotensin II and is associated
847 with human hypertension. FASEB J *24*, 1780-1788.
848
849 Oishi, Y., Manabe, I., Tobe, K., Ohsugi, M., Kubota, T., Fujiu, K., Maemura, K., Kubota,
850 N., Kadowaki, T., and Nagai, R. (2008). SUMOylation of Kruppel-like transcription
851 factor 5 acts as a molecular switch in transcriptional programs of lipid metabolism
852 involving PPAR-delta. Nat Med *14*, 656-666.
853
854 Oishi, Y., Manabe, I., Tobe, K., Tsushima, K., Shindo, T., Fujiu, K., Nishimura, G.,
855 Maemura, K., Yamauchi, T., Kubota, N., *et al.* (2005). Kruppel-like transcription factor
856 KLF5 is a key regulator of adipocyte differentiation. Cell Metab *1*, 27-39.
857
858 Parakati, R. and DiMario, J.X. (2013). Repression of myoblast proliferation and
859 fibroblast growth factor receptor 1 promoter activity by KLF10 protein. J Biol Chem

288, 13876-84.

Penn, B.H., Bergstrom, D.A., Dilworth, F.J., Bengal, E., and Tapscott, S.J. (2004). A MyoD-generated feed-forward circuit temporally patterns gene expression during skeletal muscle differentiation. Genes Dev *18*, 2348-2353.

Prosdocimo, D.A., Sabeh, M.K., and Jain, M.K. (2015). Kruppel-like factors in muscle health and disease. Trends Cardiovasc Med 25, 278-287.

Ran, F.A., Hsu, P.D., Wright, J., Agarwala, V., Scott, D.A., and Zhang, F. (2013). Genome engineering using the CRISPR-Cas9 system. Nat Protoc *8*, 2281-2308.

Relaix, F., and Zammit, P.S. (2012). Satellite cells are essential for skeletal muscle regeneration: the cell on the edge returns centre stage. Development *139*, 2845-2856.

Santolini, M., Sakakibara, I., Gauthier, M., Ribas-Aulinas, F., Takahashi, H., Kawasaki, T., Mouly, V., Concordet, J.P., Defossez, P.A., Hakim, V. and Maire, P. (2016). MyoD reprogramming requires Six1 and Six4 homeoproteins: genome-wide cis-regulatory module analysis. Nucleic Acids Res.

Sebastian, S., Faralli, H., Yao, Z., Rakopoulos, P., Palii, C., Cao, Y., Singh, K., Liu, Q.C., Chu, A., Aziz, A.*, et al.* (2013). Tissue-specific splicing of a ubiquitously expressed transcription factor is essential for muscle differentiation. Genes Dev *27*, 1247-1259.

884 Segales, J., Islam, A.B., Kumar, R., Liu, Q.C., Sousa-Victor, P., Dilworth, F.J., Ballestar,
885 E., Perdiguero, E., and Munoz-Canoves, P. (2016). Chromatin-wide and transcriptome
886 profiling integration uncovers p38alpha MAPK as a global regulator of skeletal muscle
887 differentiation. Skelet Muscle *6*, 9.
888
889 Shimizu, N., Yoshikawa, N., Ito, N., Maruyama, T., Suzuki, Y., Takeda, S., Nakae, J.,
890 Tagata, Y., Nishitani, S., Takehana, K., Sano, M., Fukuda, K., Suematsu, M., Morimoto,
891 C. and Tanaka, H. (2011). Crosstalk between glucocorticoid receptor and nutritional
892 sensor mTOR in skeletal muscle. Cell Metab *13*, 170-182.
893
894 Shindo, T., Manabe, I., Fukushima, Y., Tobe, K., Aizawa, K., Miyamoto, S.,
895 Kawai-Kowase, K., Moriyama, N., Imai, Y., Kawakami, H., *et al.* (2002). Kruppel-like
896 zinc-finger transcription factor KLF5/BTEB2 is a target for angiotensin II signaling and
897 an essential regulator of cardiovascular remodeling. Nat Med *8*, 856-863.
898
899 Sun, R., Chen, X., and Yang, V.W. (2001). Intestinal-enriched Kruppel-like factor
900 (Kruppel-like factor 5) is a positive regulator of cellular proliferation. J Biol Chem *276*,
901 6897-6900.
902
903 Sunadome, K., Yamamoto, T., Ebisuya, M., Kondoh, K., Sehara-Fujisawa, A., and
904 Nishida, E. (2011). ERK5 regulates muscle cell fusion through Klf transcription factors.
905 Dev Cell *20*, 192-205.
906
907 Takeda, N., Manabe, I., Uchino, Y., Eguchi, K., Matsumoto, S., Nishimura, S., Shindo,

908 T., Sano, M., Otsu, K., Snider, P., *et al.* (2010). Cardiac fibroblasts are essential for the
909 adaptive response of the murine heart to pressure overload. J Clin Invest *120*, 254-265.
910
911 Tatsumi, R., Anderson, J.E., Nevoret, C.J., Halevy, O., and Allen, R.E. (1998). HGF/SF
912 is present in normal adult skeletal muscle and is capable of activating satellite cells. Dev
913 Biol *194*, 114-128.
914
915 Umansky, K.B., Gruenbaum-Cohen, Y., Tsoory, M., Feldmesser, E., Goldenberg, D.,
916 Brenner, O., and Groner, Y. (2015). Runx1 Transcription Factor Is Required for
917 Myoblasts Proliferation during Muscle Regeneration. PLoS Genet *11*, e1005457.
918
919 Watanabe, N., Kurabayashi, M., Shimomura, Y., Kawai-Kowase, K., Hoshino, Y.,
920 Manabe, I., Watanabe, M., Aikawa, M., Kuro-o, M., Suzuki, T., *et al.* (1999). BTEB2, a
921 Kruppel-like transcription factor, regulates expression of the SMemb/Nonmuscle
922 myosin heavy chain B (SMemb/NMHC-B) gene. Circ Res *85*, 182-191.
923
924 Yanagi, M., Hashimoto, T., Kitamura, N., Fukutake, M., Komure, O., Nishiguchi, N.,
925 Kawamata, T., Maeda, K., and Shirakawa, O. (2008). Expression of Kruppel-like factor
926 5 gene in human brain and association of the gene with the susceptibility to
927 schizophrenia. Schizophr Res *100*, 291-301.
928
929 Yang, X.O., Doty, R.T., Hicks, J.S., and Willerford, D.M. (2003). Regulation of T-cell
930 receptor D beta 1 promoter by KLF5 through reiterated GC-rich motifs. Blood *101*,
931 4492-4499.

Zhang, Y., Liu, T., Meyer, C.A., Eeckhoute, J., Johnson, D.S., Bernstein, B.E., Nusbaum, C., Myers, R.M., Brown, M., Li, W., *et al.* (2008). Model-based analysis of ChIP-Seq (MACS). Genome Biol *9*, R137.

Zhu, N., Gu, L., Findley, H.W., Chen, C., Dong, J.T., Yang, L., and Zhou, M. (2006). KLF5 Interacts with p53 in regulating survivin expression in acute lymphoblastic leukemia. J Biol Chem *281*, 14711-14718.

942 **Figure legends**

943

944 **Figure 1**

945 **Klf5 is upregulated during myogenesis**

946 A. Relative mRNA expression of *Klf5*, *Pax7*, *Myod1*, *Myog* and *Myh3* (embryonic
947 myosin heavy chain) in intact and regenerating TA muscles. The animals were sacrificed
948 on day 4 after CTX injection. Data are means ± SEM. Representative data from three
949 individual mice are shown.

950 B. Klf5 expression during muscle regeneration. Klf5 was not detectable in quiescent
951 satellite cells (SCs) in intact muscle (arrows in the top panels). During muscle
952 regeneration, Klf5 was highly expressed in the nuclei of differentiating myocytes
953 expressing Myog (arrowheads) and regenerating myofibers, whereas Klf5 expression
954 was not detected or detected very weakly in Pax7-positive SCs (arrows). Representative
955 data from at least three individual mice are shown. Scale bar represents 20 μm.

956 C. Plated SCs were cultured in growth medium (GM) or differentiating medium (DM;
957 for 2 days or 4 days) after isolation and were co-immunostained for Klf5 with Pax7 or
958 Myog. Klf5 is expressed in the differentiating myocytes, which were negative or very
959 weakly positive for Pax7 (arrows). Klf5 was upregulated during differentiation and
960 frequently co-localized with Myog. After 4 days of culture, Klf5 levels were decreased
961 in the nuclei of large myotubes (arrowheads). Representative data from at least three
962 individual mice are shown. Scale bar represents 50 μm.

963

964 **Figure 2**

965 **Klf5 is required for muscle regeneration *in vivo***

CTX was injected into the TA muscles of SC-specific *Klf5* knockout mice (*Pax7*$^{CE/+}$;*Klf5*$^{flox/flox}$) and control *Pax7*$^{+/+}$;*Klf5*$^{flox/flox}$ mice. The animals were then sacrificed on day 4 (A), 7 (B-D) or 28 (E-F) after CTX injection.

A. *Pax7*, *Myod1*, *Myog* and *Myh3* expression in regenerating TA muscle (on day 4 after CTX injection) was analyzed using qRT-PCR (A). Data represent means ± SEM. n=3 for each group. **p<0.01. N.S., not significant.

B-F. Sections were stained with H&E or immunostained for eMyHC, laminin and collagen I. Representative images of muscle sections on day 7 (B) or 28 (E) after CTX injection are shown. The eMyHC-positive area 7 days after CTX injection was quantified using Olympus cellSense Digital Imaging software (C). Distributions of myofiber diameters on days 7 (D) and 28 (F) after CTX injection are shown. Representative data from four *Klf5* knockout and five control (for day 7) or four mice for each genotype (for day 28) are shown. Scale bars represent 100 μm.

Figure 3

Klf5 is essential for muscle differentiation

A. Establishment of *Klf5* knockout (KO) myoblasts using a CRISPR-Cas9 system. *Klf5* KO C2C12 cells or Control cells were immunostained for MyHC and Klf5 or myogenin. *Klf5* KO cells do not express Klf5 during muscle differentiation and exhibit severely reduced myotube formation. MyHC: myosin heavy chain, Myog: myogenin. Scale bar represents 100 μm.

B. Percentage of Myog-positive cells among total cells. *Klf5* KO cells exhibited less Myog expression than Control. Data are means ± SEM. (***p<0.001) Representative data from at least three individual experiments are shown.

C. Western blots showing reduced MyHC and Myog expression in *Klf5* KO C2C12 cells during differentiation. Representative data from at least three individual experiments are shown.

D. *Klf5* KO cells were infected with a Retro-viral vector (RV-Klf5) harboring *Klf5* or empty vector (RV-control), after which differentiation was induced for 2 or 4 days. The cells were then fixed and immunostained for Klf5 or MyHC. Impairment of myotube formation, as evidence from the loss of MyHC expression in *Klf5* KO cells was rescued by exogenous Klf5 expression. Representative data from at least three individual experiments are shown.

E-F. Western blots revealing the reduction of MyHC and Myog expression in *Klf5* KO C2C12 cells and its rescue by RV-Klf5. The expression levels were normalized to β-Tubulin (F). Data represent means ± SEM. (**$p<0.01$) Representative data from at least three individual experiments are shown.

Figure 4

Transient *Klf5* knockdown results in a repression of the myogenic program

A. Hierarchical clustering and heatmap of the expression levels (log2 normalized counts) of genes involved in the Hallmark Myogenesis (hallmark gene sets M5909) in C2C12 myoblasts transfected with control or *Klf5*-specific siRNA after induction of differentiation for the indicated times.

B. Functional annotations associated with genes that were inhibited in *Klf5* knockdown cells.

C. Relative distribution of RNA-seq tags of genes with MyoD binding during the course of myoblast differentiation. Box-and-whisker plot showing log2 counts of the

MyoD-regulated genes and the remaining RefSeq genes normalized to the counts in control siRNA-transfected cells on day 0. *P* values are between control siRNA (Ctrl) and siKlf5 (KD) cells analyzed using the Mann-Whitney *U* test.

D. MA plot depicting the relationship between fold changes in myotube differentiation-related genes, comparing RNA-seq from differentiating myoblasts transfected with control siRNA or siRNA targeting Klf5. Red dots represent genes with MyoD binding, and the Gray dots represents genes without MyoD binding.

E. UCSC genome browser images illustrating normalized RNA-seq reads for the representative myogenesis-related genes *Myog* and *Myl4* in control or Klf5 siRNA-transfected C2C12 cells at the indicated days after induction of differentiation.

F. Relative mRNA expression of *Klf5*, *Myog*, *Mybph*, *Myl4* and *Myom2* in C2C12 cells transfected with control siRNA or siRNA targeting Klf5. Data represent means ± SEM. (*p<0.05, **p<0.01, ***p<0.001, n=3, biological replicates.)

G. *de novo* motifs identified in regions bound by MyoD in myotubes. The enrichment for a known Sp1 motif was also analyzed.

Figure 5

Klf5 regulates myogenesis-related target genes in concert with MyoD

A. UCSC genome browser images illustrating normalized tag counts for Klf5 (post-differentiation day 0, 2, 5), MyoD (myotube, differentiated for 2 days) and Mef2D (myotube, differentiated for 5 days) at *Myog* loci in differentiating C2C12 myotubes.

B. Heatmap for binding of Klf5 (post-differentiation day 0, 2, and 5), MyoD (myotubes, differentiated for 2 days) and Mef2D (myotubes, differentiated for 5 days) within 2 kb around the center of the top 1000 Klf5-binding sites on day 5. The Klf5 binding sites

were subdivided into 2 groups based on the presence of significant MyoD binding peaks in myotubes within 500 bp of the Klf5 binding regions. The distribution of Klf5 tag densities in each subgroup were shown as histogram.

C. Distribution of Klf5 tag densities in the vicinity of MyoD-bound loci in myoblasts differentiated for 0, 2 and 5 days.

D. Distribution of Klf5 tag densities in the vicinity of Mef2D-bound loci in myoblasts differentiated for 0, 2 and 5 days.

E. Venn diagram showing the overlap between the 12,769 MyoD peaks, 11,193 Mef2D peaks and 4,382 Klf5 peaks identified by ChIP-seq. Note over half the Klf5 peaks (2,224 out of 4,382 peaks) are also bound by MyoD and/or Mef2.

F. Direct interaction of Klf5 and MyoD or Mef2 shown by co-immunoprecipitation. Whole cell extract from C2C12 cells differentiated for 5 days were immunoprecipitated using anti-MyoD or anti-Mef2 antibody. The interaction between Klf5 and MyoD or Mef2 is shown compared to the 1% Input or control samples without primary antibodies.

G. *de novo* motifs identified in regions bound by Klf5 in myotubes after differentiation for 5 days.

H. HEK-293T cells were co-transfected with *Myog*-luciferase; Klf5, MyoD, and Mef2D expression plasmids, as indicated; and a control CMV-renilla luciferase plasmid. Luciferase activities relative to the basal level of *Myog*-luciferase cotransfected with empty expression vectors are shown. Data represent means ± SEM. (**$p<0.01$, ***$p<0.001$, ****$p<0.0001$). Representative data from three individual experiments are shown.

Figure 6

MyoD function is inhibited in *Klf5*-null C2C12 myoblasts

A. UCSC genome browser images illustrating normalized tag counts for MyoD at *Myod1*, *Myog*, *Myl4* and *Mybph* gene loci in GFP-targeted control (orange) or *Klf5*-null (red) C2C12 myotubes differentiated for 3 days.

B. Distribution of MyoD tag densities in the vicinity of MyoD-bound enhancers in the GFP-targeted control or *Klf5*-null C2C12 myotubes differentiated for 3 days.

C. Comparison of MyoD recruitment at E-box containing enhancers of the *Myog, Mybph, Myom2* and *Myl4* gene loci in the GFP-targeted control and *Klf5* null C2C12 myotubes differentiated for 3 days. Data represent means ± SEM. (**p<0.01, ***p<0.001, n=3, biological replicates).

Figure 7

Klf5 is required for satellite cell differentiation

A. Isolated SCs from Klf5 knockout mice ($Pax7^{CE/+}$;$Klf5^{flox/flox}$) were cultured in the presence or absence of 4OH-Tmx in growth medium for 2 days. Purified protein derived from primary myotubes differentiated for 3 days were analyzed by western blotting. Representative blots from three individual experiments are shown.

B. Relative mRNA expression of *Myog Myl4 and Myom2* in SCs differentiated for 3 days. Data represent means ± SEM (**p<0.01). Representative data from three individual experiments are shown.

Supplementaly figure legends

Figure 1- figure supplement 1

Preparation of SC primary cultures.

A. Isolated EDL myofibers with their associated SCs were immediately fixed and immunostained for Pax7 and Klf5.

B. SCs were prepared from EDL muscles from wild-type C57/B6 mice and stained for Pax7 and MyoD.

C-D. Proportion of $Pax7^+$, $Pax7^+$: $MyoD^+$ and $MyoD^+$ cells (C) or $Pax7^+$, $Pax7^+$: $Klf5^+$ and $Klf5^+$ cells (D) in the primary SCs cultured in the growth media (GM). Expression of MyoD in every analyzed cells, indicating these cells are composed of pure, myoblast-lineage population. $Pax7^+$: $MyoD^-$ cells was not detected.

E. Two days post differentiation, propotion of $Myog^+$, $Myog^+$: $Klf5^+$ and $Klf5^+$ cells were analyzed. Note that all the Myog positive cells were also positive for Klf5. Data represent means ± SEM. Representative data from at least three individual mice are shown. DM: differentiation medium.

Figure2 - figure supplement 1

Tamoxifen treatment does not affect TA muscle morphology.

TA muscles were obtained from Klf5 knockout mice ($Pax7^{CE/+}$; $Klf5^{flox/flox}$) and control $Pax7^{+/+}$; $Klf5^{flox/flox}$ mice on day 28 after tamoxifen injection. Muscle morphology was assessed by H-E staining.

Figure 3- figure supplement 1

Klf5 knockdown impairs myoblast differentiation.

A. *Klf5* expression during C2C12 differentiation. Bars depict means ± SEM. n=3, biological replicates. GM: growth medium, DM: differentiation medium.

B. Induction of Klf5 expression during C2C12 differentiation was assessed immunostaining for MyHC and Klf5. Klf5 is highly expressed in the nuclei of differentiating myoblasts expressing MyHC and in myotubes. However, little Klf5 expression was seen in proliferating C2C12 cells in GM. Representative data from at least three individual experiments are shown. MyHC: Myosin heavy chain. Scale bar represents 100 μm.

C. Relative mRNA expression of Klf family members in C2C12 myotube on day 3 by QPCR. Bars depict means ± SEM. n=3, biological replicates.

Figure 3- figure supplement 2

Establishment of _Klf5_ knockout C2C12 cells.

A. C2C12 cells were transfected with pSpCas9-Klf5 or GFP-targeted control vector. After puromycin selection, the cells were cloned using the limiting dilution method. Three *Klf5* knockout (KO) clones and three control C2C12 clones were obtained. *Klf5* KO was confirmed by the absence of immunofluorescence. Compared to the control cells, all *Klf5* KO cells exhibited defective myotube formation, as indicated by MyHC staining. Scale bar represents 100 μm.

B. Confirmation of mutation in the *Klf5* gene locus. The position of guide RNA is indicated by the blue boxes. The red boxes indicate deleted sequences in the mutant allele, and the white # in the red box indicates the substituted nucleotide in the mutant allele. Clones #1 and #3 have a 1-bp deletion mutation in both alleles. The one allele of

the clone #2 contains a 33-bp deletion, and the other allele contains a 33-bp deletion plus a 1-bp substitution mutation.

Figure 3- figure supplement 3

Phenotype of *Klf5* knockdown cells.

A-C. Klf5, myogenin (Myog), and MyHC expression in C2C12 cells after siRNA treatment. C2C12 cells were treated with either siKlf5 or siControl (siCtrl). After siRNA treatment in GM for 24 h, the medium was replaced with DM. After 2 days in DM, the cells were fixed and co-immunostained. Note the ratio of Myog-positive cell was significantly decreased by siKlf5 treatment (B). Data represent means ± SEM. (*$p<0.05$) Representative data from at least three individual experiments are shown.

D. Fusion index indicating fibers containing more than 3 nuclei. The fusion index was significantly reduced in cells transfected with siKlf5, though similar levels of MyoD positivity was detected. Data represent means ± SEM. (***$p<0.001$) Representative data from at least three individual experiments are shown. Scale bar represents 100 μm. N.D.: not detected.

E. Growth curve of siCtrl- and siKlf5-treated C2C12 cells in GM. Data represent means ± SEM. Representative data from four individual experiments are shown.

Figure 5- figure supplement 1

Klf5, MyoD and Mef2D are colocalized in the myogenesis-related gene loci.

UCSC genome browser images illustrating normalized tag counts for Klf5 (post differentiation day 0, 2, 5), MyoD (myotubes, differentiated for 2 days) and Mef2D (myotubes, differentiated for 5 days) at *Myod1, Mybph* and *Myl4* loci in C2C12

myotubes.

Figure5-figure supplement 2

MyoD and Klf5 are recruited to the E-box-containing enhancer of the *Myog* locus

Recruitment of MyoD (A), Klf5 (B) and Mef2 (C) to the *Myog* promoter was monitored using ChIP assays with chromatin prepared from C2C12 myoblasts after differentiation for 0, 2 or 5 days. The *Gapdh* locus served as a negative control. n=3, biological replicates.

Figure5-figure supplement 3

Klf5 binding regions in undifferentiated myoblasts

Heatmap for binding of Klf5 (post-differentiation day 0, 2, and 5), MyoD (myotubes, differentiated for 2 days) and Mef2D (myotubes, differentiated for 5 days) within 2 kb around the center of the top 1000 Klf5-binding sites on day 0. The Klf5 binding sites were subdivided into 2 groups based on the presence of significant MyoD binding peaks in myotubes within 500 bp of the Klf5 binding regions. The distribution of Klf5 tag densities in each subgroup were shown as histogram.

Figure 6- figure supplement 1

Levels of MyoD and Mef2 protein were not altered by Klf5 deletion.

Levels of MyoD, Mef2, Klf5 and Myog protein were analyzed by Western blotting using GFP-targeted control or *Klf5* knockout myoblasts differentiated for 5 days. Representative data from four individual experiments are shown.

Figure 6-figure supplement2

MyoD function is inhibited in *Klf5*-null C2C12 myoblasts -analysis in the another set of control and *Klf5*-null cells

A. UCSC genome browser images illustrating normalized tag counts for MyoD at *Myog*, *Myl4*, *Mybph* and *Myod1* gene loci in GFP-targeted control or *Klf5*-null C2C12 myotubes differentiated for 3 days.

B. Distribution of MyoD tag densities in the vicinity of MyoD-bound enhancers in GFP-targeted control or *Klf5*-null C2C12 myotubes differentiated for 3 days.

Figure 4-source data 1

Gene ontology analysis on the genes upregulated by *Klf5* knockdown

Functional annotations associated with genes that were induced >1.5-fold with *Klf5* knockdown at day 3 post differentiation.

Supplementary File 1.

Table 1: list of oligonucleotides

Table 2: list of antibodies

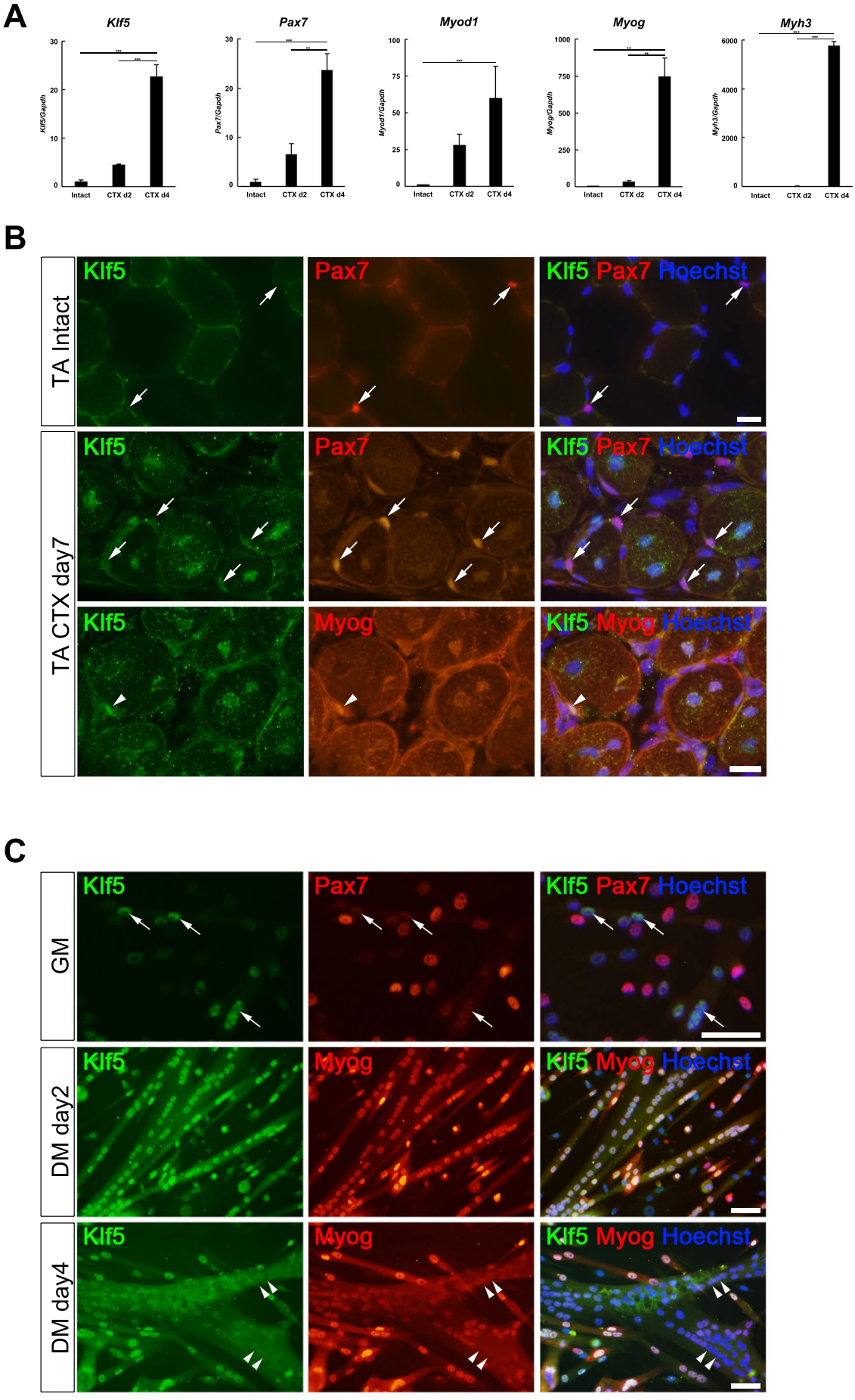

Hayashi et al. Fig 1

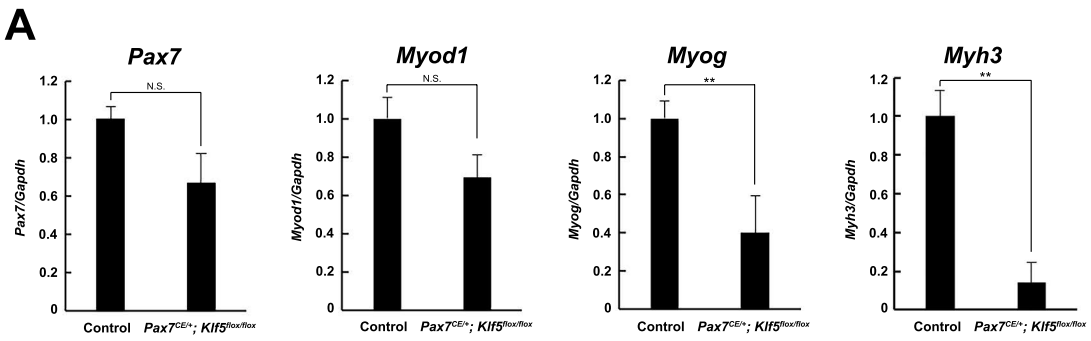

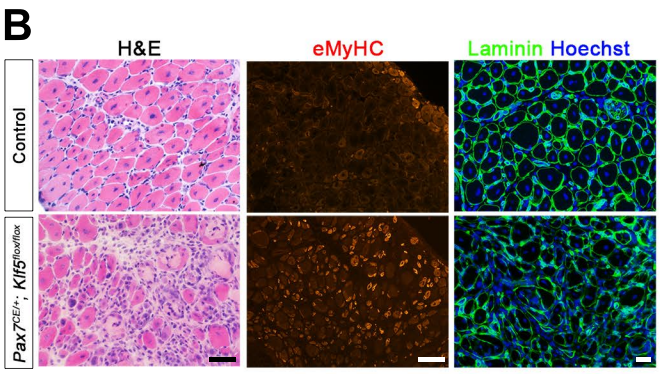

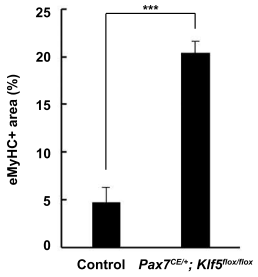

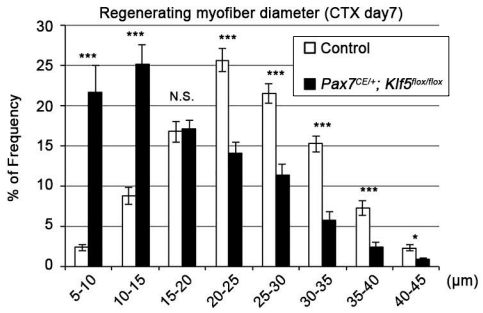

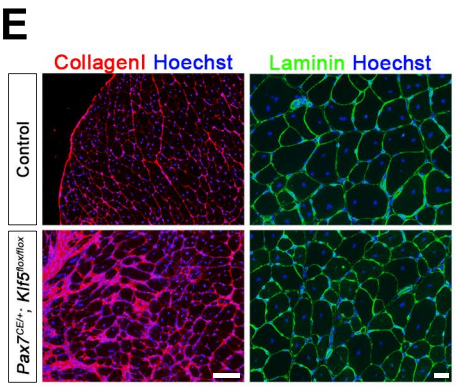

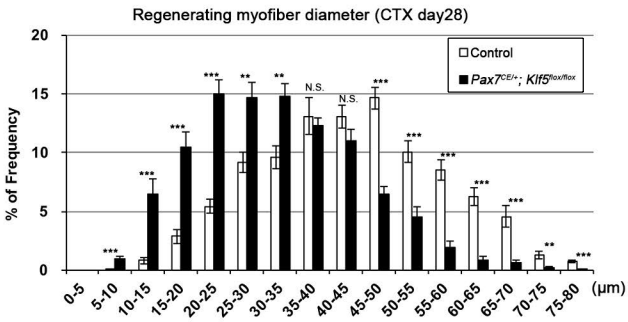

Hayashi et al. Fig 2

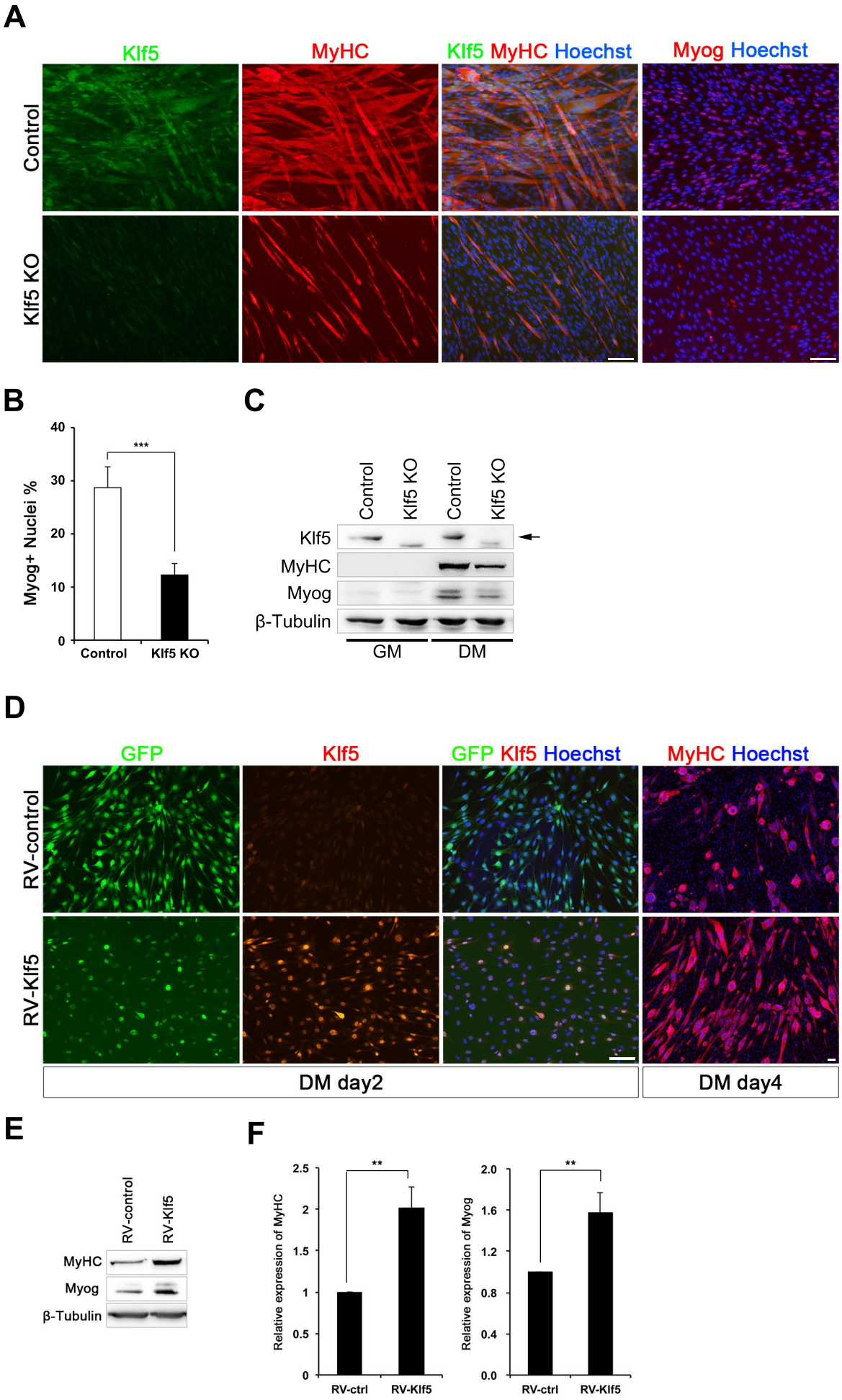

Hayashi et al. Fig 3

A

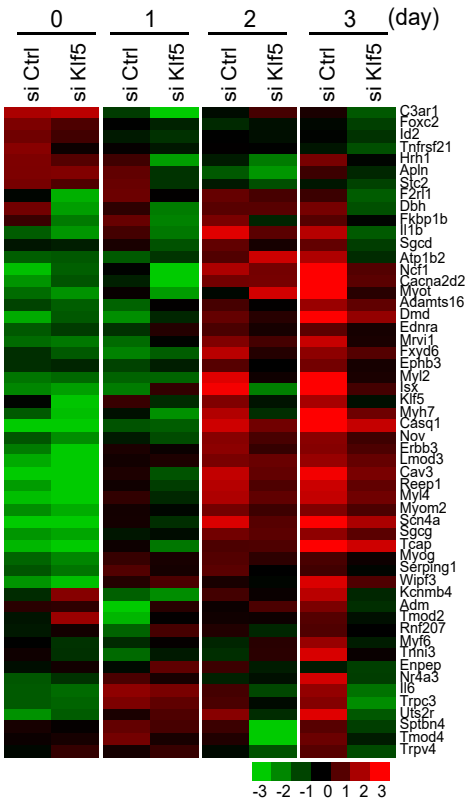

B

GO Description	%	Log_{10} (p)
HALLMARK MYOGENESIS	2.73	-7.60
HALLMARK GLYCOLYSIS	2.49	-6.05
actin filament-based process	5.39	-5.87
regulation of nervous system development	6.13	-5.77
Hypertrophic cardiomyopathy (HCM)	1.41	-5.52
extracellular matrix organization	3.73	-5.36
muscle cell development	1.99	-5.02

C

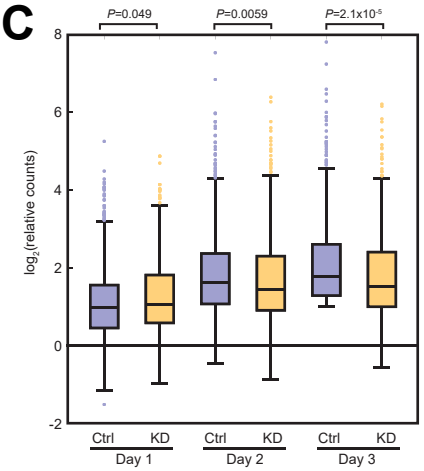

D

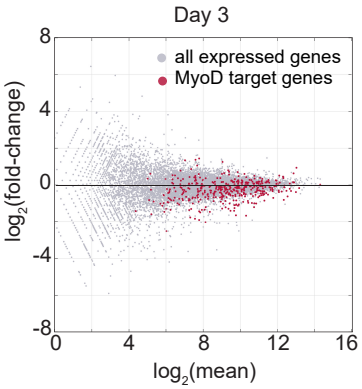

E

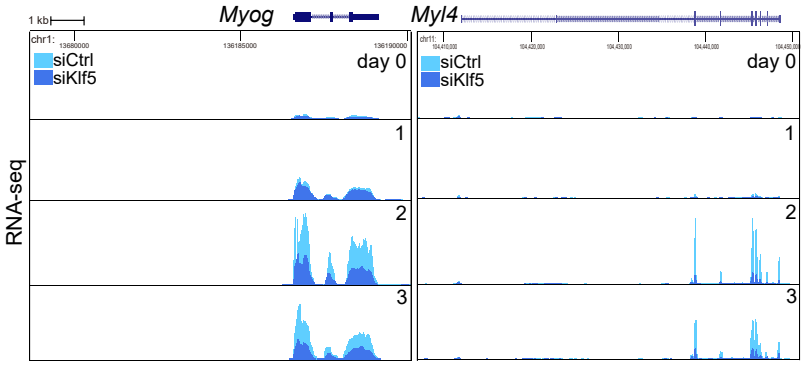

F

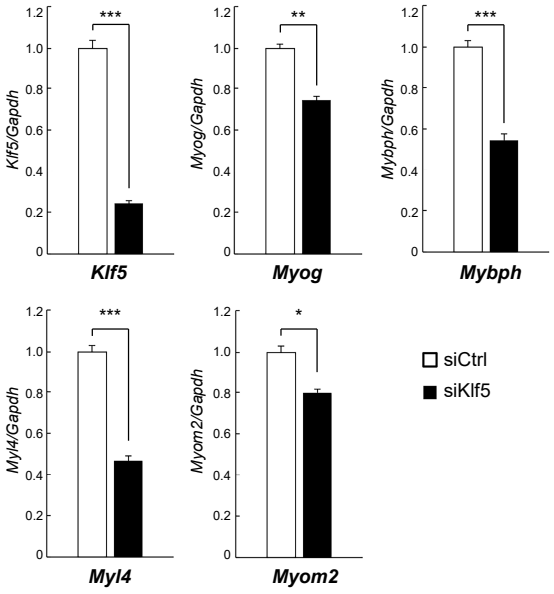

G

rank	motif	name	p-value	% of targets
1		MyoD (bHLH)	1e-2829	79.3%
2		Pbx3 (Homeobox)	1e-95	27.5%
3		Fosl2 (bZIP)	1e-87	9.80%
4		Klf5 (zinc finger)	1e-44	11.3%
6		MEF2	1e-25	1.61%
		Sp1	1e-19	4.90%

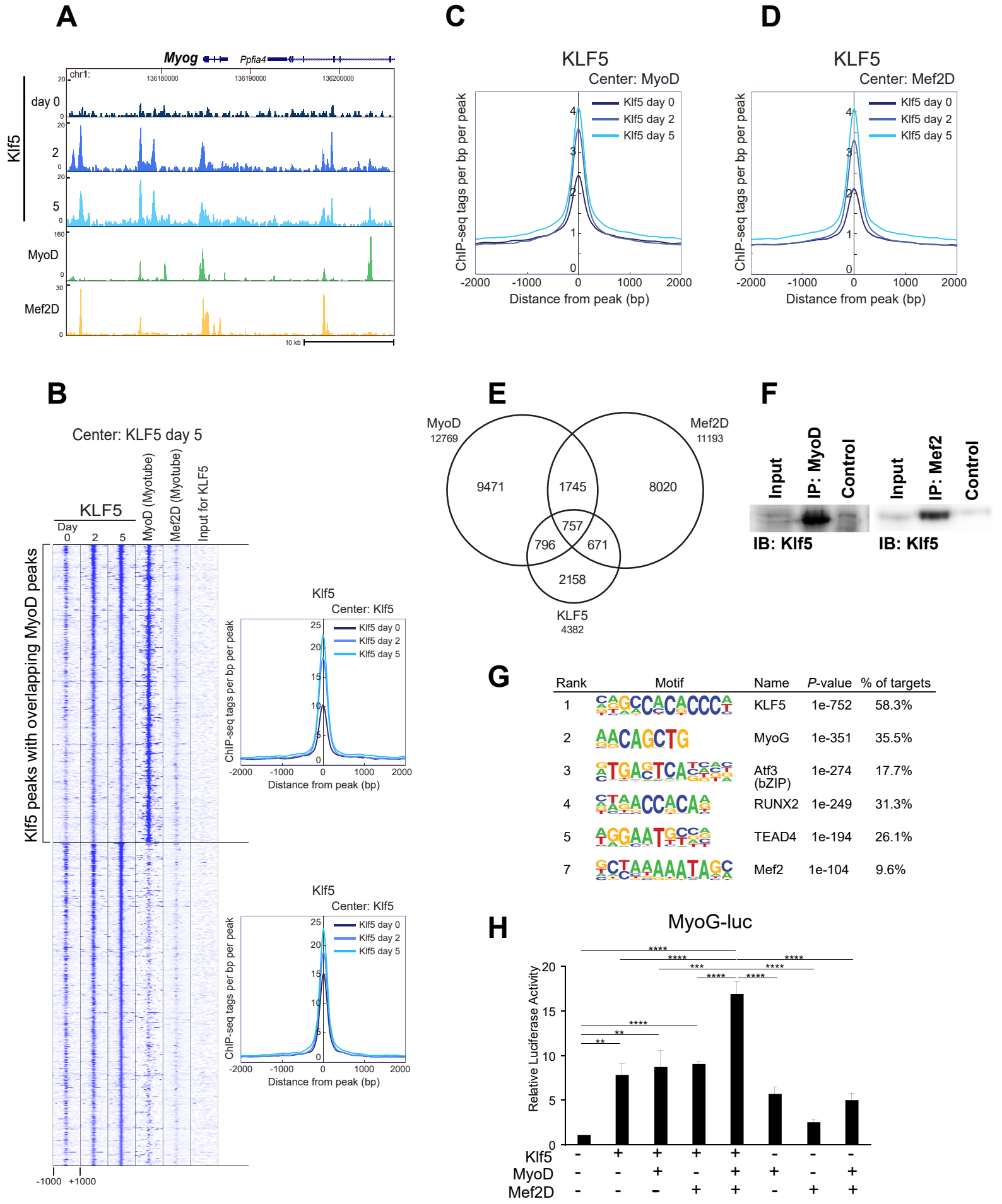

Hayashi et al_Fig 5

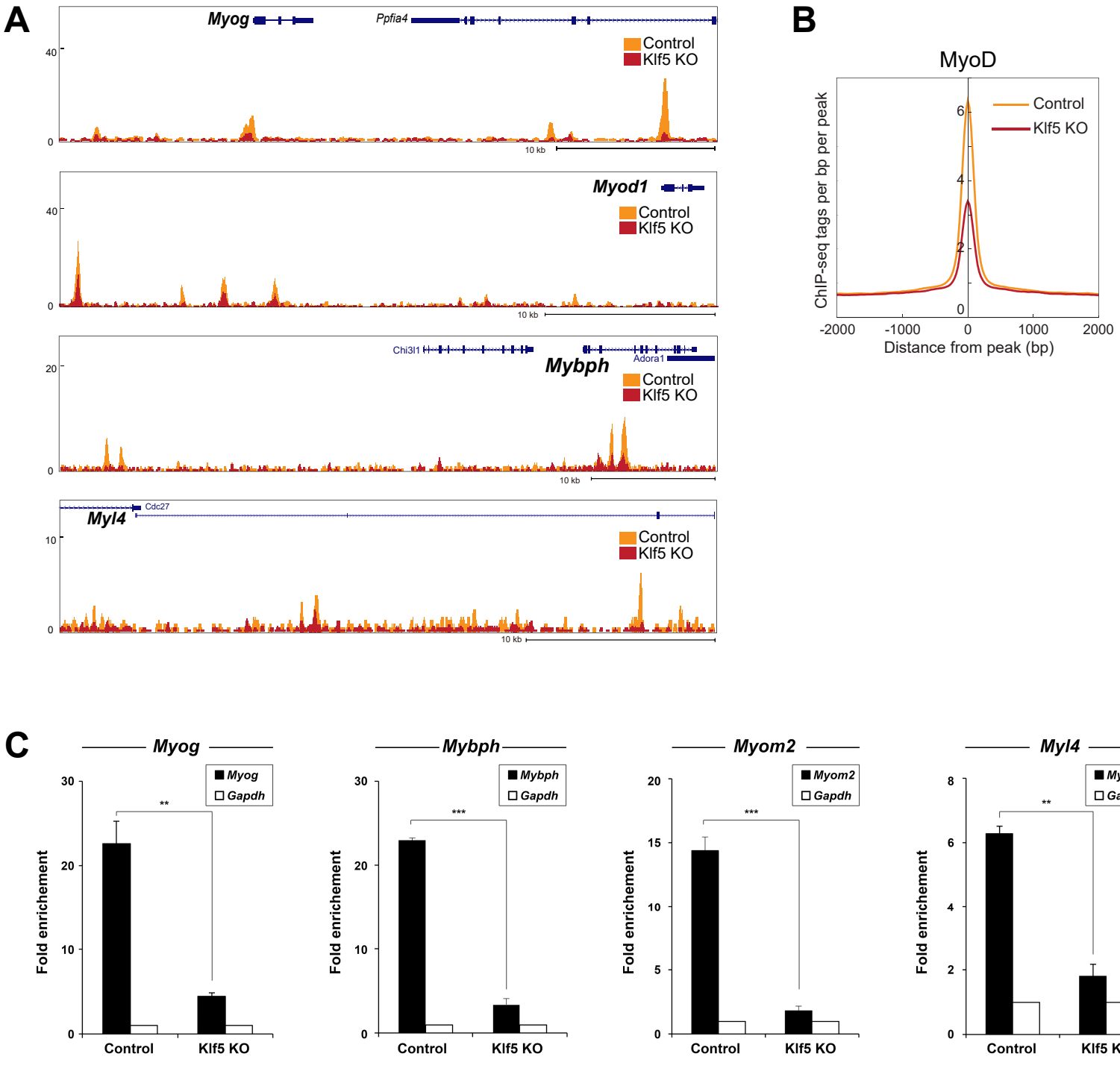

Hayashi et al. Fig. 6

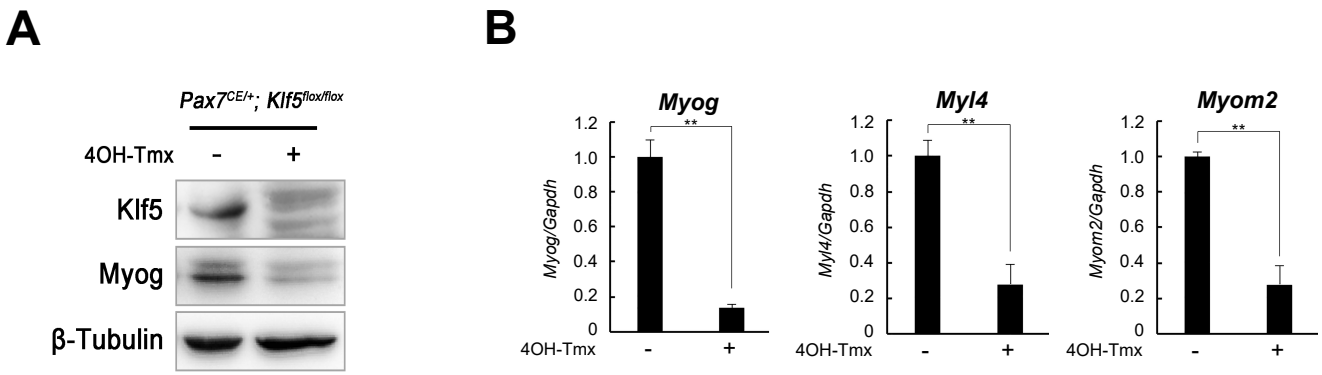

Hayashi et al. Fig. 7

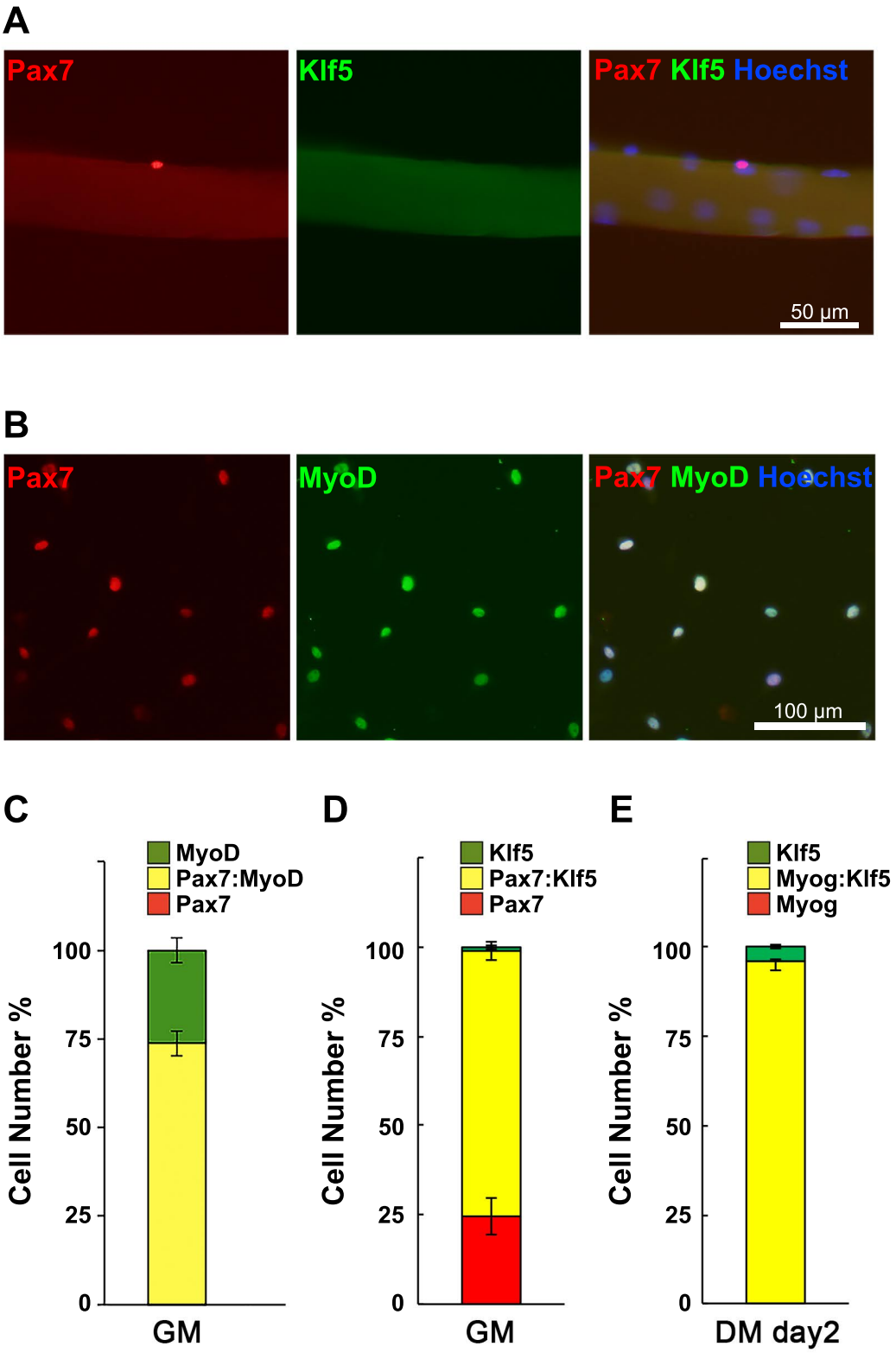

Hayashi et al. Figure 1-figure supplement 1

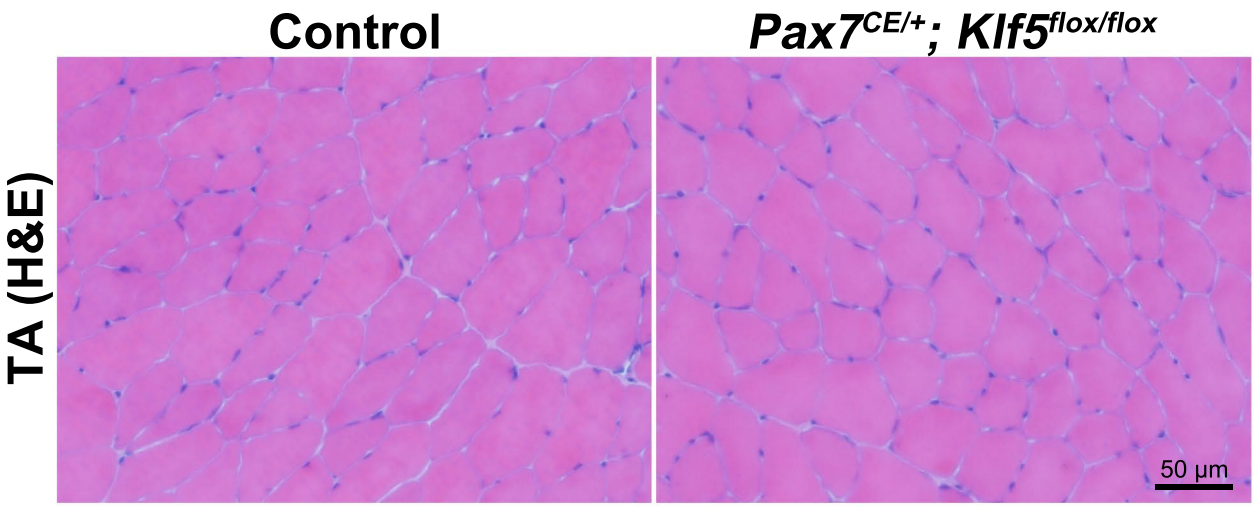

Hayashi et al. Figure 2 - figure supplement 1

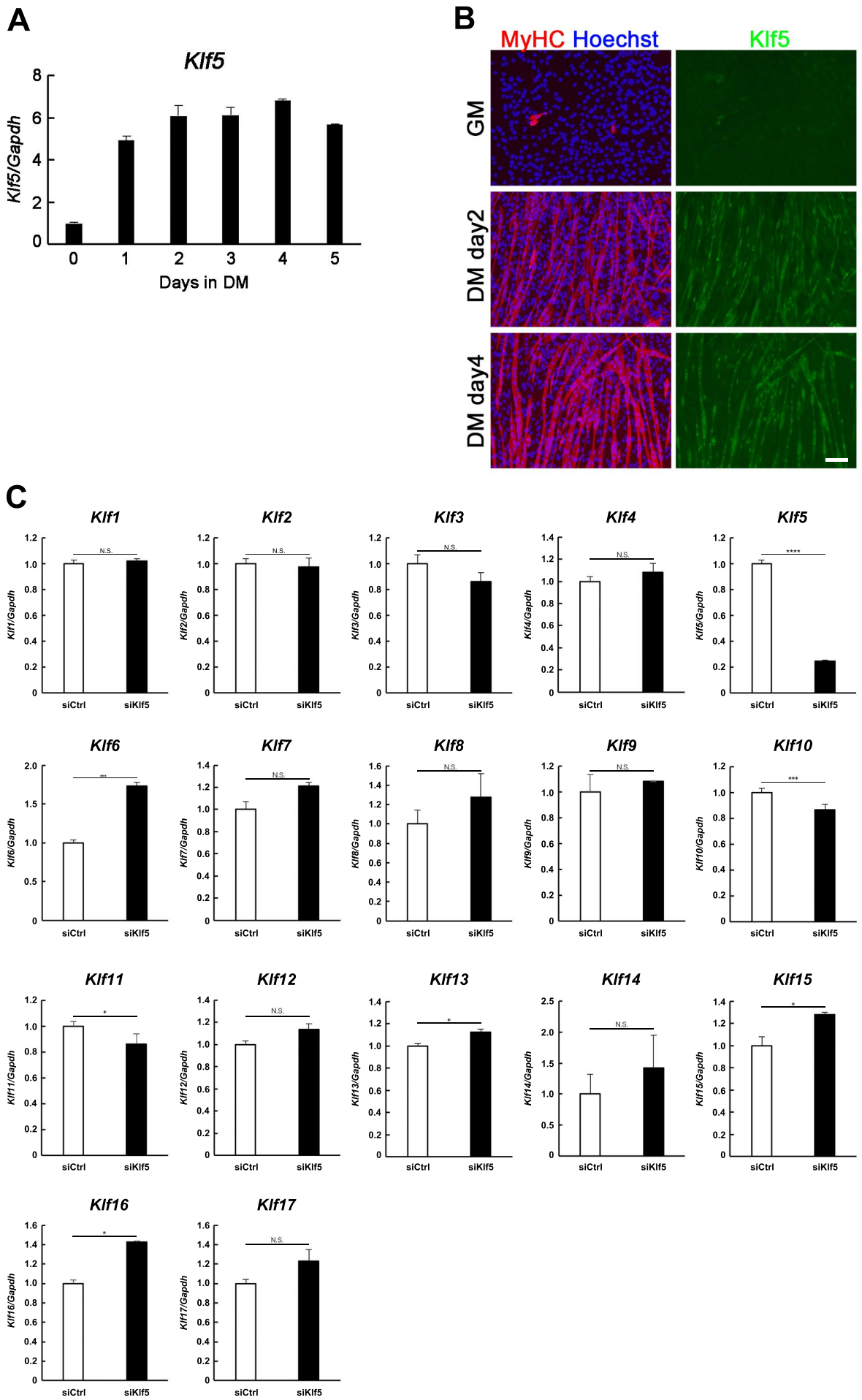

Hayashi et al. Figure 3 - figure suplement 1

A

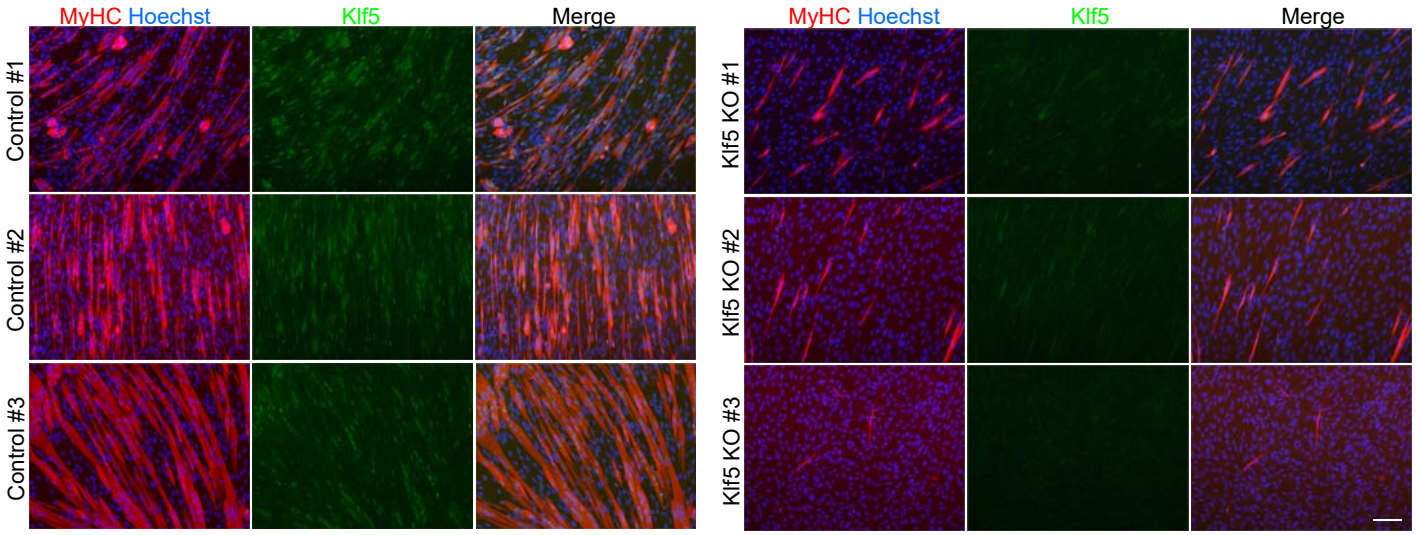
MyHC Hoechst
Klf5
Merge
Control #1
Control #2
Control #3
MyHC Hoechst
Klf5
Merge
Klf5 KO #1
Klf5 KO #2
Klf5 KO #3

B

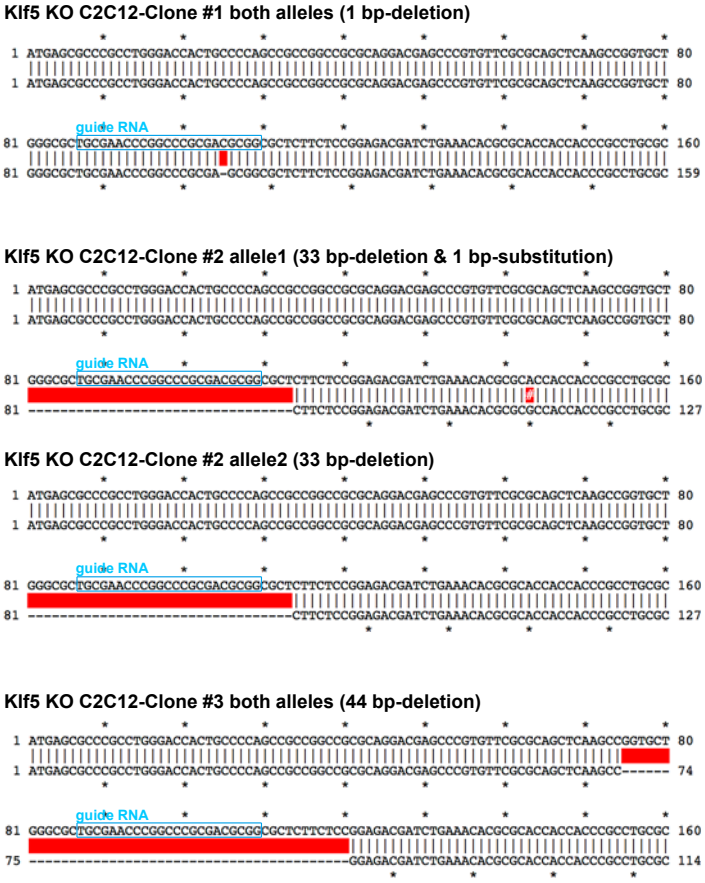
Klf5 KO C2C12-Clone #1 both alleles (1 bp-deletion)
1 ATGAGCGCCCGCCTGGGACCACTGCCCCAGCCGCCGGCCGCGCAGGACGAGCCCGTGTTCGCGCAGCTCAAGCCGGTGCT 80
1 ATGAGCGCCCGCCTGGGACCACTGCCCCAGCCGCCGGCCGCGCAGGACGAGCCCGTGTTCGCGCAGCTCAAGCCGGTGCT 80
guide RNA
81 GGGCGCTGCGAACCCGGCCCGCGACGCGGCGCTCTTCTCCGGAGACGATCTGAAACACGCGCACCACCACCCGCCTGCGC 160
81 GGGCGCTGCGAACCCGGCCCGCGA-GCGGCGCTCTTCTCCGGAGACGATCTGAAACACGCGCACCACCACCCGCCTGCGC 159
Klf5 KO C2C12-Clone #2 allele1 (33 bp-deletion & 1 bp-substitution)
1 ATGAGCGCCCGCCTGGGACCACTGCCCCAGCCGCCGGCCGCGCAGGACGAGCCCGTGTTCGCGCAGCTCAAGCCGGTGCT 80
1 ATGAGCGCCCGCCTGGGACCACTGCCCCAGCCGCCGGCCGCGCAGGACGAGCCCGTGTTCGCGCAGCTCAAGCCGGTGCT 80
guide RNA
81 GGGCGCTGCGAACCCGGCCCGCGACGCGGCGCTCTTCTCCGGAGACGATCTGAAACACGCGCACCACCACCCGCCTGCGC 160
81 ----------CTTCTCCGGAGACGATCTGAAACACGCGCGCCACCACCCGCCTGCGC 127
Klf5 KO C2C12-Clone #2 allele2 (33 bp-deletion)
1 ATGAGCGCCCGCCTGGGACCACTGCCCCAGCCGCCGGCCGCGCAGGACGAGCCCGTGTTCGCGCAGCTCAAGCCGGTGCT 80
1 ATGAGCGCCCGCCTGGGACCACTGCCCCAGCCGCCGGCCGCGCAGGACGAGCCCGTGTTCGCGCAGCTCAAGCCGGTGCT 80
guide RNA
81 GGGCGCTGCGAACCCGGCCCGCGACGCGGCGCTCTTCTCCGGAGACGATCTGAAACACGCGCACCACCACCCGCCTGCGC 160
81 ----------CTTCTCCGGAGACGATCTGAAACACGCGCACCACCACCCGCCTGCGC 127
Klf5 KO C2C12-Clone #3 both alleles (44 bp-deletion)
1 ATGAGCGCCCGCCTGGGACCACTGCCCCAGCCGCCGGCCGCGCAGGACGAGCCCGTGTTCGCGCAGCTCAAGCCGGTGCT 80
1 ATGAGCGCCCGCCTGGGACCACTGCCCCAGCCGCCGGCCGCGCAGGACGAGCCCGTGTTCGCGCAGCTCAAGCC------ 74
guide RNA
81 GGGCGCTGCGAACCCGGCCCGCGACGCGGCGCTCTTCTCCGGAGACGATCTGAAACACGCGCACCACCACCCGCCTGCGC 160
75 ----------GGAGACGATCTGAAACACGCGCACCACCACCCGCCTGCGC 114

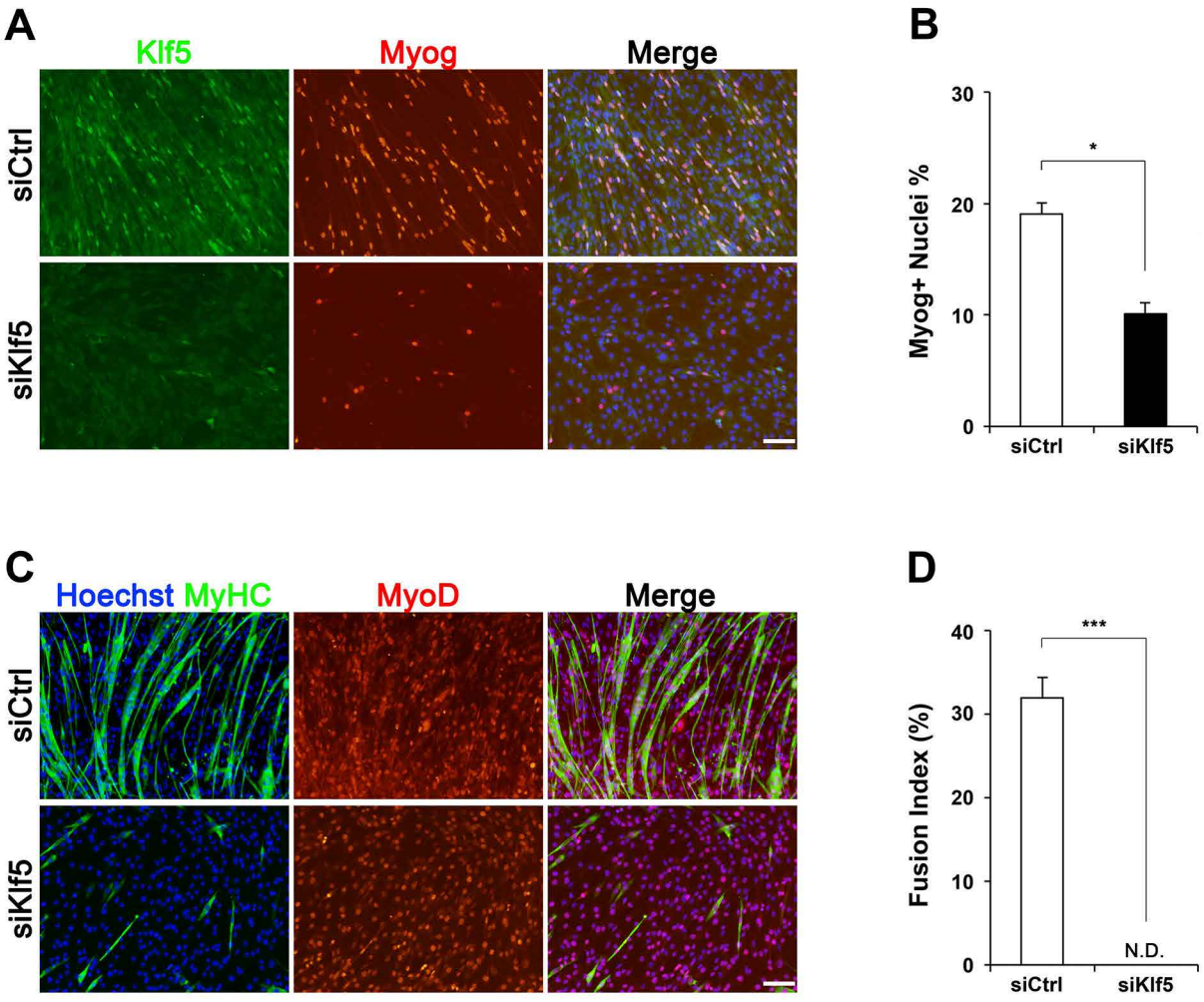

Hayashi et al. Figure 3 - figure supplement 3

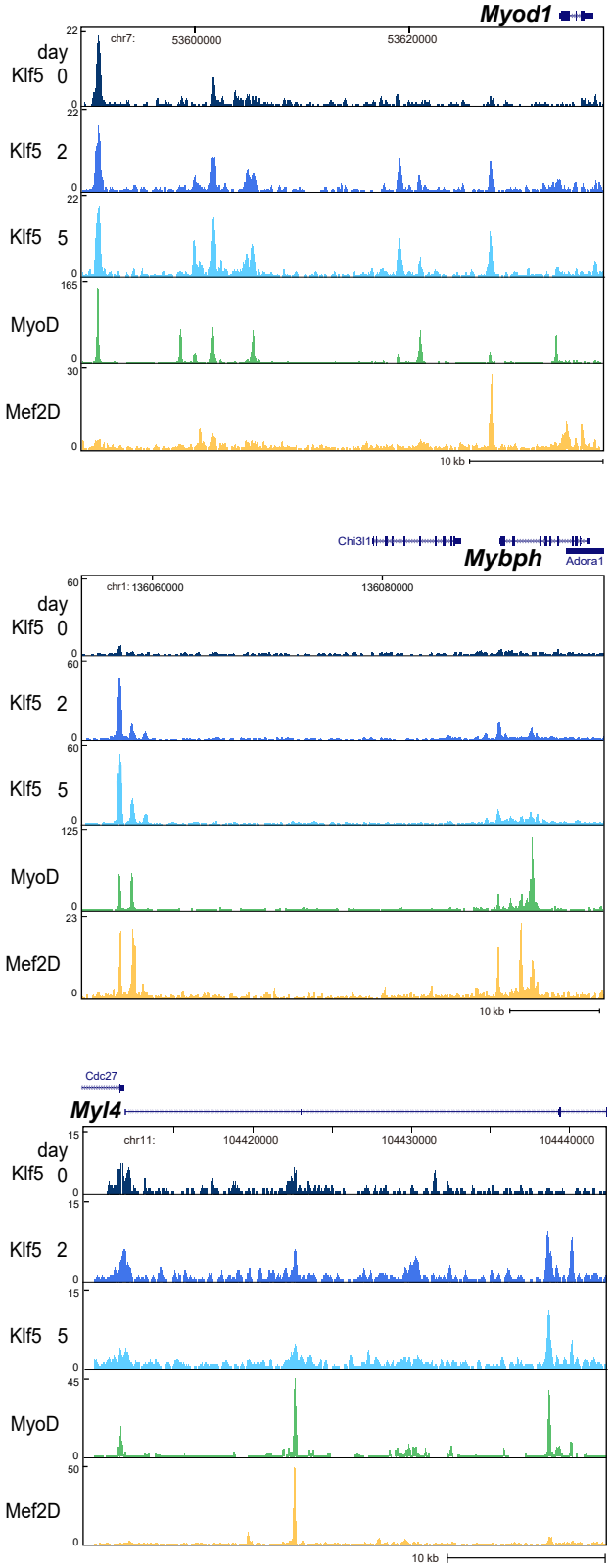

Hayashi et al. Figure 5 - figure supplement 1

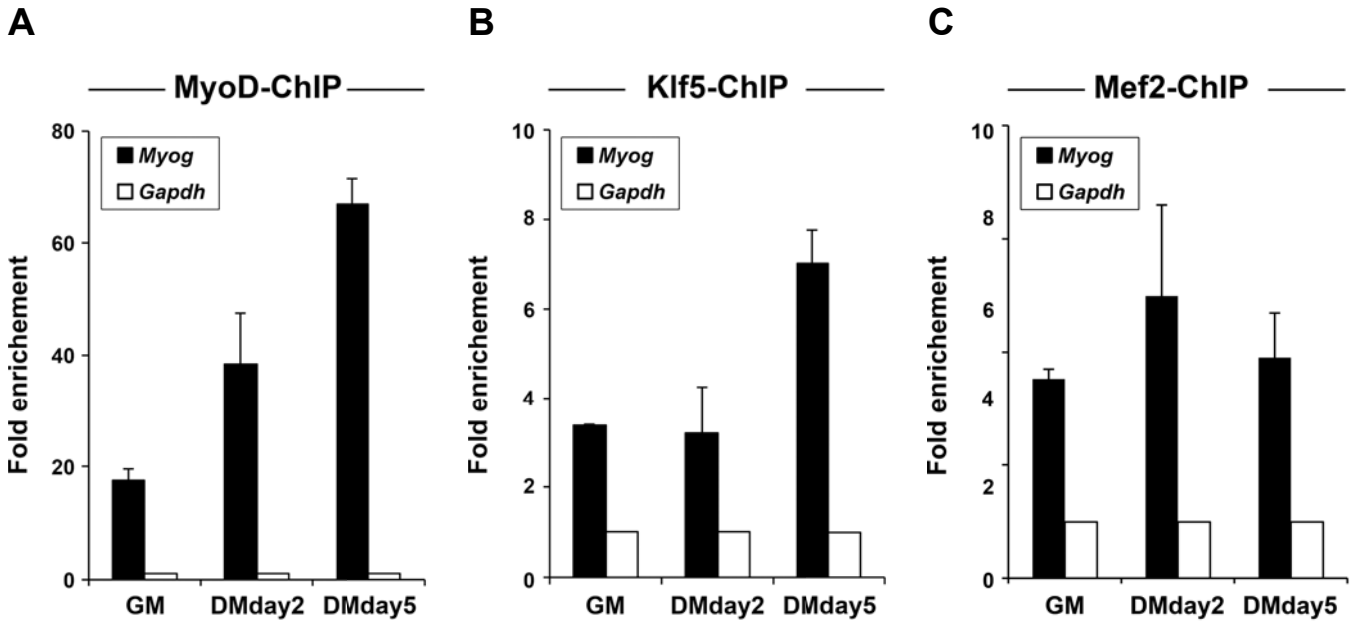

Hayashi et al. Figure 5-figure supplement 2

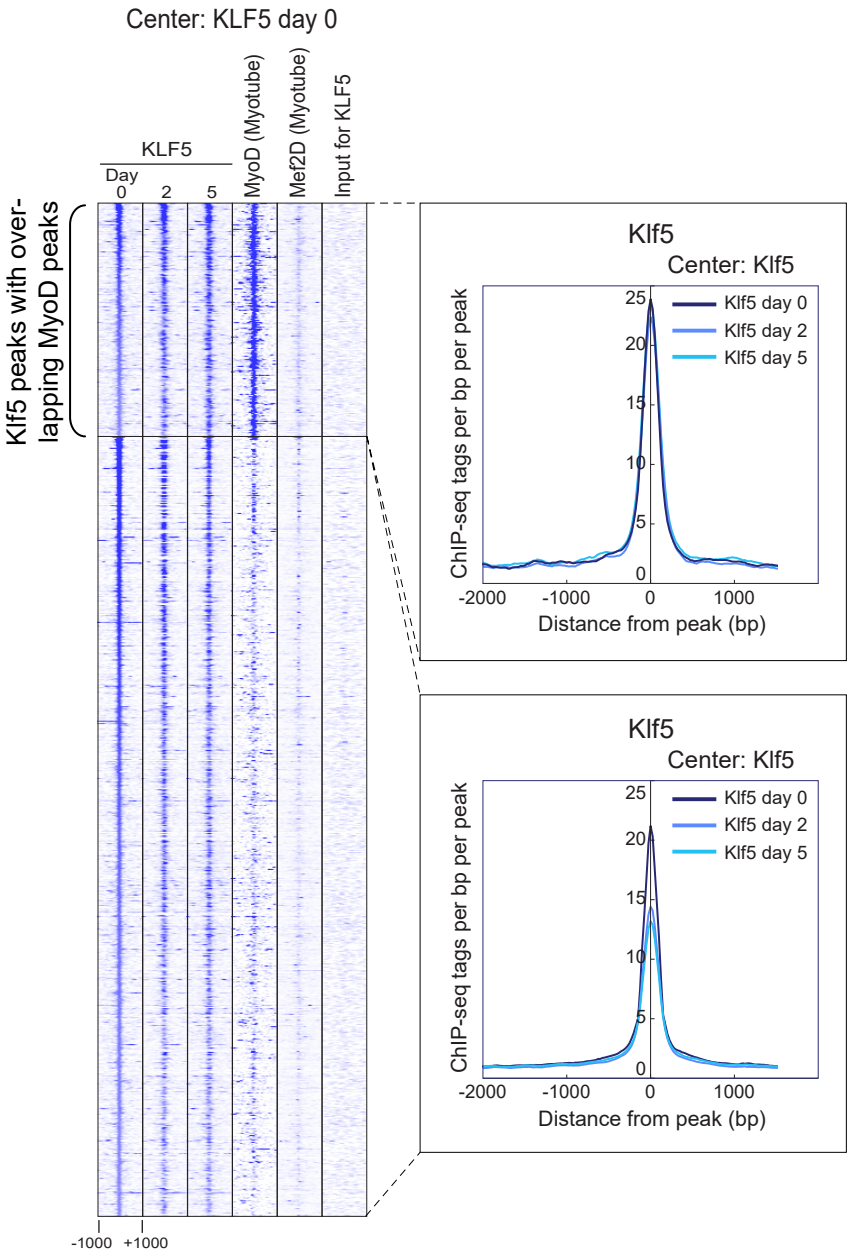

Hayashi et al. Figure 5-figure supplement 3

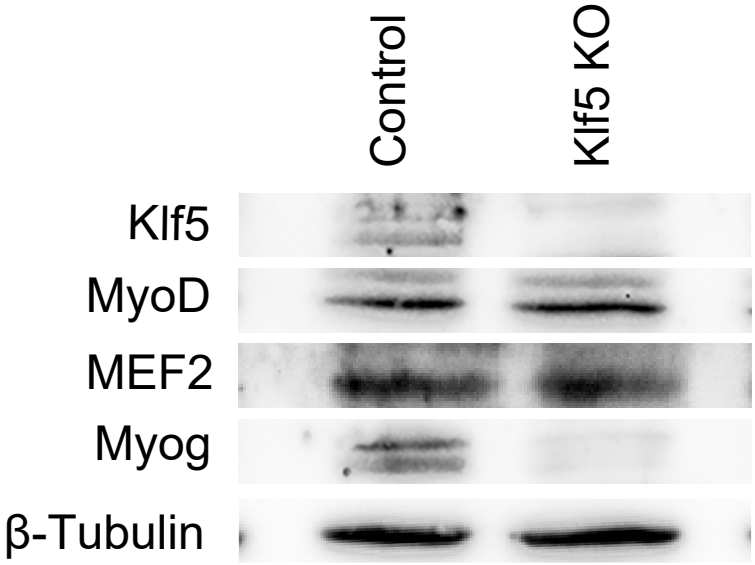

Hayashi et al. Figure 6 - figure supplement 1

A

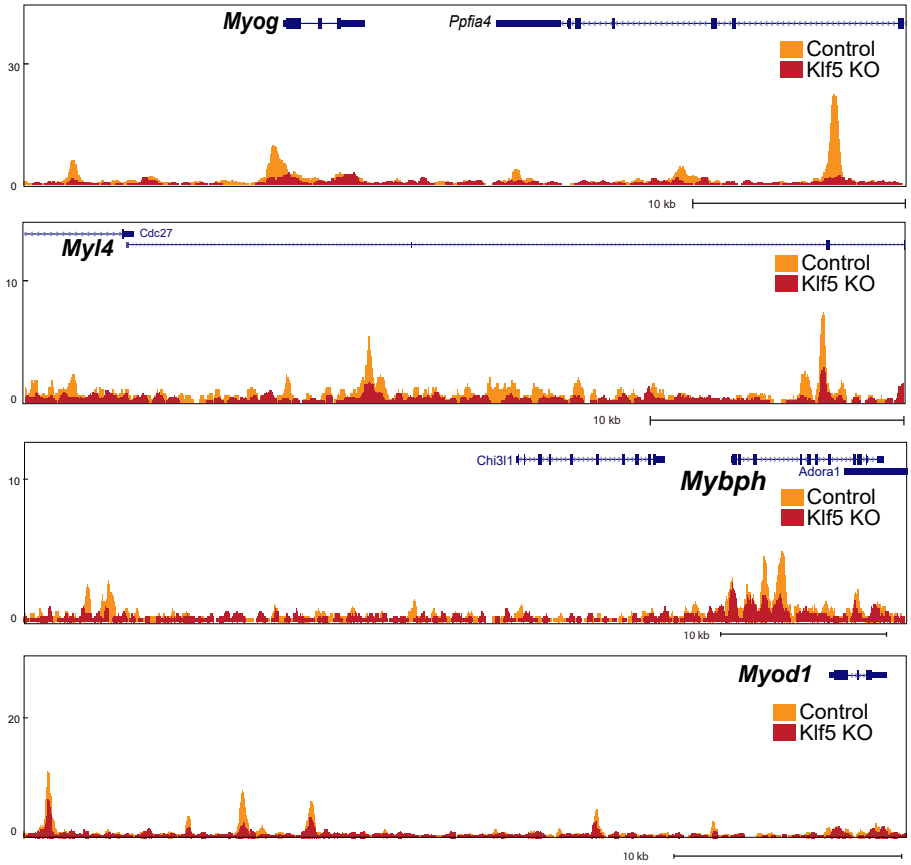

B

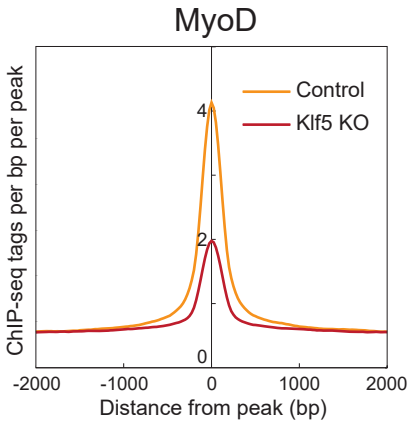

Hayashi et al. Figure 6 - figure supplement 2